IEEE Access
Multidisciplinary | Rapid Review | Open Access Journal

Received May 11, 2020, accepted May 25, 2020, date of publication June 5, 2020, date of current version June 29, 2020.

*Digital Object Identifier 10.1109/ACCESS.2020.3000420*

# A Robust Strategy Based on Marine Predators Algorithm for Large Scale Photovoltaic Array Reconfiguration to Mitigate the Partial Shading Effect on the Performance of PV System

**DALIA YOUSRI[1], THANIKANTI SUDHAKAR BABU[2], (Member, IEEE), EMAN BESHR[3], MAGDY B. ETEIBA[1], AND DALIA ALLAM[1]**

[1]Electrical Engineering Department, Faculty of Engineering, Fayoum University, Faiyum 63514, Egypt
[2]Department of Electrical Power Engineering, Institute of Power Engineering, Universiti Tenaga Nasional, Kajang 43000, Malaysia
[3]Electrical and Control Engineering Department, Arab Academy for Science, Technology, and Maritime Transport, Cairo 11311, Egypt

Corresponding author: Eman Beshr (beshre@aast.edu)

**ABSTRACT** Large-scale solar photovoltaic (PV) plants play an essential role in providing the increasing demand for energy in recent time. Therefore, in the purpose of achieving the highest harvested power under the partial shading conditions as well as protecting the PV array from the hot-spot calamity, the PV reconfiguration strategy is established as an efficient procedure. This is performed by redistribution of PV modules according to their levels of shading. Motivated by this, the authors in this article have introduced a novel population-based algorithm that is known as marine predators algorithm (MPA) to restructure the PV array dynamically. Moreover, a novel objective function is introduced to enhance the algorithm performance rather than utilizing the regular weighted objective function in the literature. The effectiveness of the proposed algorithms based on the novel objective function is evaluated using several metrics such as fill factor, mismatch losses, percentage of power loss, and percentage of power enhancement. Besides, the obtained results are compared with a regular total-cross-tied (TCT) connection, manta ray foraging optimization (MRFO), harris hawk optimizer (HHO) and particle swarm optimizer (PSO) based reconfiguration techniques. Furthermore, to demonstrate the suitability of the proposed methods, large scale PV arrays of 16 $\times$ 16 and 25 $\times$ 25 are considered and evaluated. The results reveal that MPA enhanced the PV array power by percentage of 28.6 %, 2.7 % and 5.7 % in cases of 9 $\times$ 9, 16 $\times$ 16 and 25 $\times$ 25 PV arrays, respectively. The comprehensive comparisons endorse that MPA shows a successful shade dispersion; hence the number of multiple peaks in the PV characteristics has reduced, and high values of power have been harvested with least mean execution time in comparison with PSO, HHO and MRFO. Moreover, the Wilcoxon signed-rank test has been accomplished to confirm the reliability and applicability of the proposed approach for the PV large scale arrays as well.

**INDEX TERMS** Renewable energy, energy efficiency, PV reconfiguration, partial shading, marine predators algorithm, partial shading, optimization.

## I. INTRODUCTION

In recent years, research on extraction of maximum power from a photovoltaic (PV) system has been focused on dynamic change of irradiation and temperature conditions [1], [2]. This enhanced power generation helps to maximize the efficiency of a PV plant and reduces the cost per unit of power generation. Among the various renewable energy resources, solar PV has attained high priority because of its abundance and availability throughout the year. In addition, solar PV has been widely used in various applications and it is preferred widely in remote locations. The efficiency of solar PV decreases because of factors such as irradiation, temperature, non-linearity of PV, and partial shading. Partial shading occurs mainly because of passing clouds, building shadows, dust and bird droppings, manufacturing defects,

The associate editor coordinating the review of this manuscript and approving it for publication was Huiqing Wen.

and nonuniform aging of PV modules [3]. Because of partial shading, the power generated by PV systems installed in buildings can be reduced by 5 to 10% [4], with a reduction of 3 to 6% in the case of highly rated plants [5].

To overcome the limitations of partial shading, various authors have proposed different types of maximum power extraction techniques, such as multilevel inverter based maximum power point tracking (MPPT) [6], distributed MPPT techniques [7]–[9], and algorithmic based DC-DC converter MPPT [10]–[12]. These methods performed well in individual. However, each method has limitations. For example, inverter based and distributed MPPT techniques require a complex control system, and each PV module used an individual inverter will increase costs [7], [13]. To overcome these limitations, array configuration techniques were introduced in [14]–[16]. Among the previously discussed methods, PV array configuration is the most economical and extensively used method. The various basic configuration techniques are series, parallel, series-parallel (SP), total-cross-tied (TCT), honeycomb (HC) and bridge-link (BL) [17]. The authors in [18], followed a probabilistic approach to reduce shade losses for SP, TCT, and BL configurations. In [19], by analyzing various performance parameters among above said methods, the authors confirmed that the TCT configuration gives superior performance and minimizes mismatch losses in comparison with the basic configurations. However, the major drawback in TCT is that, the output current generated by the PV array is limited, when the maximum number of PV modules in row are shaded [20]. With this motivation, the authors proposed various reconfiguration techniques, such as adaptive, static, and dynamic reconfiguration, to diffuse the shade equally over the entire PV array. This enhances power generation and reduces the mismatch losses.

In [21], the authors proposed an adaptive reconfiguration technique to lower the partial shading effect. In this technique, the PV array is separated into adaptive and fixed parts through a switching matrix. This follows a simpler control technique; however, the authors failed to propose this method for a greater number of re-configurable columns. In addition, this method requires high number of current and voltage sensors and switches. This increase the system's cost [22]. To minimize cost and complexity, static reconfiguration techniques were introduced. The notable static reconfiguration techniques are Su Do Ku [22], optimal Su Do Ku [23], improve Su Do Ku, futoshiki [24], competence square (CS) [25], dominance square (DS) [26], and the Zig-Zag scheme [27]. Other innovative rearrangements for fixed reconfiguration are presented in [28], [29]. Furthermore, an optimal fixed reconfiguration technique is proposed by reducing row spacing between arrays in [30]. Another method based on an odd-even structure for TCT-configured systems is presented in [31]. A new static reconfiguration technique for $5 \times 5$ PV array is proposed in [32].

In static techniques, the reconfiguration takes place based on puzzles. As per the puzzle output, the positions of the PV modules will be interchanged without altering electrical connections. Therefore, these methods require lengthy cables, more skilled technicians, and laborious work. Because of this, these methods are not preferred in real time, even though they achieve the best performance.

Dynamic and electrical array reconfiguration techniques were also introduced to reduce the partial shading effect. In these techniques, the reconfiguration of PV modules takes place based on the switching signals received from the switching matrix. According to the switching signals, the connections between PV modules will be interchanged without altering the physical locations of the PV modules. This technique is implemented at first for grid-connected PV application in [14]. It works based on principle of reducing the index of irradiance equalization. Another dynamic reconfiguration technique based on the irradiance equalization method is presented in [33]. In [20], the reconfiguration is treated as a mixed integer quadratic programming problem, and a branch-and-bound algorithm is used to find the optimal reconfigured pattern. This method is time consuming and fails to implement in real-time applications. The authors in [34] introduced rough set theory to dynamically reconfigure the SP connected PV array to maximize the power generation. Improved dynamic programming methods, such as the smart choice algorithm and munkres assignment algorithm, were discussed in [35] for effective reconfiguration.

Further, to improve the effectiveness of the dynamic reconfiguration techniques and for extraordinary improvement of meta-heuristic optimization algorithms, speaks to the driving force behind the search for optimal reconfiguration of PV modules. With this motivation, authors have introduced optimization-based reconfiguration techniques for the application of PV, namely, genetic-algorithm (GA) [16], particle swarm optimization (PSO) [36], and the grasshopper optimization algorithm [1], and different schemes based on evolutionary algorithms are proposed in [20]. In [16], [36], the authors reconfigured the partially shaded PV modules in an array in such a way that the current difference between rows of the PV array is minimized. Therefore, the power generation can be enhanced. The previously discussed methods exhibit limitations such as consuming more time for convergence to reconfigure the system. In addition, the PSO algorithm may converge prematurely and become trapped in local optima. In complex problems, defining initial parameters is difficult [37]. Furthermore, the quality of the solution deteriorates, as the population size increases in GA. Recently modified harris hawks optimizer (MHHO) has been proposed to solve these issues [38]. Whereas these algorithms have a common drawback, that is utilizing a weighted objective function to optimize the shaded PV array reconfiguration problem. With unreliable selection for the values of the weights, the algorithms are trapping with the local optimum. Therefore, authors motivated to introduce a novel objective function to tackle this issue.

Therefore, this article proposes new reconfiguration techniques to enhance maximum power generation from a PV

plant based on a novel objective function. The main outcomes of this article are as follows:

- The authors introduce a novel objective function to avoid the demerits of the weighted objective function which is commonly used in the literature.
- Two Novel population-based algorithms named marine predators algorithm (MPA) and manta ray foraging optimization MFRO) have been proposed to be applied on PV reconfiguration strategy.
- A comparison between the novel objective function and the weighted fitness function is carried out to demonstrate the impact of the novel one on the performance of the selected algorithms.
- Effectiveness of the proposed techniques is evaluated by considering two shaded patterns on $9 \times 9$ PV array.
- To verify the superiority of the proposed population-based algorithms, efficiency metrics are calculated and correlated with the TCT and other published methods.
- Large scale PV arrays in ranges of $16 \times 16$ and $25 \times 25$ have been utilized to assess the quality and reliability of the proposed approach.
- The proposed algorithm is compared with the most recently published techniques of PV reconfiguration approach, that are PSO, and HHO based on several measures including mismatch power loss, fill factor, percentage power loss, and mean execution time.
- Wilcoxon signed rank test has been accomplished among the MPA and MRFO, HHO, and PSO to assess the consistency and the reliability of the proposed technique.

The remaining sections of the manuscript are formulated as follows. Section II describes the modeling of the PV module. The representation of TCT connected PV array and its current and voltage calculations are presented in Section III. The formulation of objective function for the proposed techniques are given in Section IV. Descriptions of the proposed algorithms and implementation steps are presented in Section V. The obtained results and discussion are provided in Section VI. Extensive analysis with large scale PV array structures are presented in Section VII. Finally, the main conclusion is detailed in Section VIII.

## II. MODELING OF PV MODULE

Modeling of a solar PV cell is an essential task in its proper design which lead in turn to improving the effectiveness of the whole PV system. An accurate PV cell can emulate the real-time characteristics of any PV system. However, the PV cell modeling is a difficult task because of the cell's nonlinearity [39]. Therefore, various authors have focused on developing an accurate model that can help in improving the performance of the PV plant. By performing numerous analyses and using various optimization algorithms, researchers have developed a trio of diode PV models: the single-diode model [40], the two-diode model [41], [42], and the three-diode model [43]. Among the three diode PV models, the single-diode PV model is preferred due to its simplicity, easy of design, and less parameters involved. The electrical circuit diagram of this PV model is presented in Fig. 1, which comprises the current source $I_{pv}$ connected antiparallel to diode $D_1$, series and shunt resistance are $R_s, R_p$ respectively. Similarly, the two-diode and three-diode models consist of circuits with two and three diodes, respectively. The current generated by each PV model can be estimated by applying Kirchhoff's current law to its equivalent circuit. The total current generated by the single-diode PV model is given as follows:

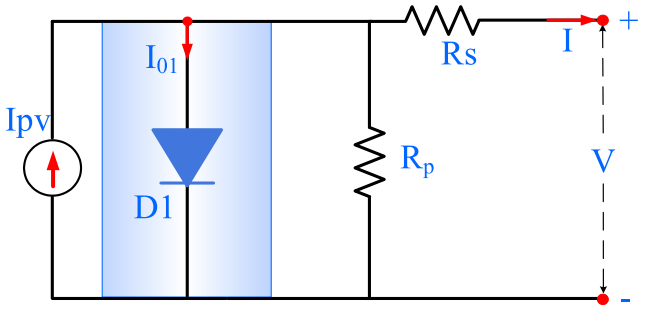


**FIGURE 1.** Electrical circuit of single diode PV model.

$$I = I_{pv} - I_{D1} - I_p \tag{1}$$

where $I_{pv}$ is the current produced by a PV source, $I_{D1}$ is a current flowing through the diode, and $I_p$ is a current across the shunt resistance.

By substituting $I_{D1}$ and $I_p$, the current equation can be written as follows:

$$I = I_{pv} - I_{01}\left(exp\left(\frac{V_{D1}}{a_1 V_t} - 1\right)\right) - \left(\frac{V + IR_s}{R_p}\right) \tag{2}$$

where $V_t$ is the thermal voltage and can be depicted as $\frac{N_s KT}{q}$, where $k$ is the Boltzmann constant $= 1.3805 - 10^{-23} J/K$, $T$ is the cell temperature in Kelvin, $q$ is the electron charge $= 1.6 - 10^{-19} C$, $N_s$ is the number of cells in series, $a_1$ is the ideality factor, and $I_{01}$ is the diode $D_1$ leakage current. The power generated by a PV system greatly depends on environmental conditions. Therefore, the current generated by a PV source can be mathematically represented as given in Eq. 3.

$$I_{pv} = \left(\frac{G}{G_0}\right)[I_{sc} + k_i(T - T_0)] \tag{3}$$

where $I_{sc}$ represents the short-circuit current at the standard test condition (STC), that is, $G_0 = 1000 W/m^2$ and $T_0 = 25°C$. $G$ and $T$ are considered actual irradiation and temperature values, respectively, and $k_i$ indicates the current coefficient factor.

## III. TCT-CONNECTED PV ARRAY

TCT is the most widely used connection scheme to achieve the required amount of power. Researchers have confirmed that a TCT-connected system shows extensive performance

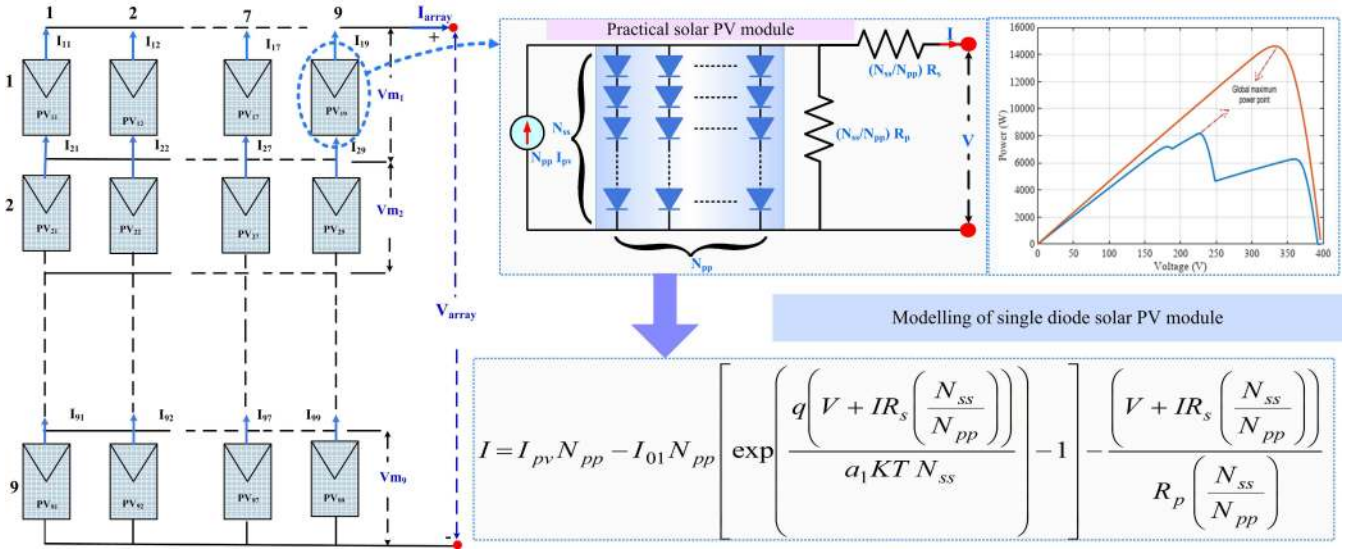


**FIGURE 2.** TCT connected 9 × 9 PV array structure and modelling of PV module with P-V characteristics.

compared with SP, HC, and BL connections [19], [20]. The TCT connection is framed by connecting cross-ties across each row of an SP configuration. In this article, the authors consider a 9 × 9 TCT PV array for verification of the proposed methods, as shown in Fig. 2. This TCT-connected system consists of 9 rows and 9 columns. Each PV module is indicated by $m$, $n$, where $m$ and $n$ indicate rows and columns, respectively.

The total current and voltage of a TCT connected system can be calculated as given in Eq. 4 and Eq. 5 for 9 × 9 array, respectively.

$$I_{R_m} = \sum_{n=1}^{9}\left(\frac{G_{mn}}{G_s} I_{M_{mn}}\right), \quad m = 1, 2, 3, \ldots, 9. \tag{4}$$

$$V_{array} = \sum_{m=1}^{9} V_{M_m} \tag{5}$$

where $I_{R_m}$ is the PV arrays current produced at row m, $V_{array}$ is the total voltage that appears across terminals of the PV array, $V_{M_m}$ and $I_{M_{mn}}$ are the PV module voltage and current at row $x$ at the standard $G_s = 1000\ \frac{W}{m^2}$), respectively.

To achieve maximum power from the considered PV array, the incident shadow should disperse regularly over the surface of the PV modules. The uniform distribution for the partial shading phenomenon cannot be satisfied by using the TCT arrangement. Moreover the number of the utilized switches in the TCT connection is so huge that reach for 2 × (M) × (M+1)−2+2×N × (M × N -M) where M, N the total number of rows and columns. Therefore, the authors motivated to propose a simpler and more flexible approach to provide the optimal switching matrix interconnection with minimal number of switches based on meta-heuristic optimization algorithms based on the depicted block diagram in Fig. 3.

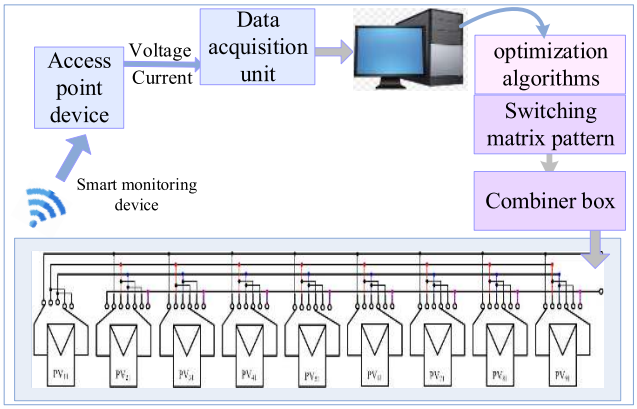


**FIGURE 3.** Structure of optimization algorithms based on switching matrix combination.

The details of the proposed algorithms and the reconfiguration optimization process are presented in the next sections.

## IV. OBJECTIVE FUNCTION DEFINITION

Defining the objective function is one of the main requirements for the optimization algorithm to start the process. For the PV array reconfiguration problem, to harvest maximum power with a regular distribution for the shadow on the PV array surface, authors proposed a novel objective function as a ratio among the total of the produced PV array power and the absolute error among the highest and lowest values of the rows current that can be framed as follows:

$$Maximize\ (obj(i)) = \frac{Array_{power}}{|I_{max} - I_{min}|} \tag{6}$$

where $obj(i)$ represents the fitness value of the $i^{th}$ element in the present population. $I_{max}$, and $I_{min}$ are the maximum and minimum values of the currents in the rows current vector I

$= [I_1, I_2, I_3, \ldots, I_9]$. $Array_{power}$ is the total array power, and it can be defined as given in Eq. 7:

$$Array_{power} = \sum_{m=1}^{X} I_{R_m} \times V_m \tag{7}$$

where $I_{R_m}$ and $V_m$ are the current and voltage of the PV array for the $m^{th}$ row, respectively. The symbol $X$ refers to the total number of the rows of the considered array, for example $X = 9$ for $9 \times 9$ PV array and 6 for $6 \times 20$ PV array.

The principle target of the proposed objective function is to maximize the harvested PV array power with minimal deviation among the maximum and minimum values of rows current to guarantee a regular shade distribution on the PV surface (one peak (P-V) characteristic will be noted).

## V. PROPOSED POPULATION-BASED ALGORITHMS

The population based algorithms have established the superiority of theirs in resolving nonlinear multi modal optimization problems as opposed with specific the conventional algorithms. So, in the present work, several innovative and techniques are applied for PV reconfiguration to appraise the responses of theirs and suggest the best method. As the no-free-lunch principle states that no entity algorithm is viewed as a great method for every search engine optimization disputes [44], which motivated the authors to check many population based algorithms. The specifics and implementation of the proposed algorithms for the application PV reconfiguration are discussed in the following subsections.

### A. MARINE PREDATORS ALGORITHM

The marine predators algorithm (MPA) is a fairly recent suggested algorithm inspirited by the actions of predator and prey in nature [45]. In MPA, the prey as well as predator are viewed as search representatives, since the predator searching for the prey, meanwhile the prey itself looking for its food. MPA is equally as all of the meta heuristic techniques (MHs) began by arbitrary set of solutions as an initialization. Then those solutions are customized based upon the primary framework of the algorithm.

The initial solutions are determined randomly dependant on the search space as follows;

$$Z = LB + r_1 \times (UB - LB) \tag{8}$$

where, the $LB$ and $UB$ refer to the upper and lower borders in the search landscaping, $r_1 \in [0, 1]$ is the arbitrary number.

As explained early, the prey and predator in MPA are considered as search agents therefore there are two primary matrices named best/elite matrix (matrix of probably the fittest predators) and also the prey matrix must be identified. The defined two matrices are usually represented mathematically as follows:

$$Elite = \begin{bmatrix} Z^1_{11} & Z^1_{12} & \ldots & Z^1_{1d} \\ Z^1_{21} & Z^1_{22} & \ldots & Z^1_{2d} \\ \ldots & \ldots & \ldots & \ldots \\ Z^1_{n1} & Z^1_{n2} & \ldots & Z^1_{nd} \end{bmatrix}, \tag{9}$$

$$Z = \begin{bmatrix} Z_{11} & Z_{12} & \ldots & Z_{1d} \\ Z_{21} & Z_{22} & \ldots & Z_{2d} \\ \ldots & \ldots & \ldots & \ldots \\ Z_{n1} & Z_{n2} & \ldots & Z_{nd} \end{bmatrix}, \tag{10}$$

Finding optimal solutions is the primary goal of MHs. Therefore the first arbitrary set of solutions are updated depending on the algorithm structure. The velocity ratio among the predator and the prey is the main factor in transmitting the algorithm from phase to another. In MPA, the large-velocity ratio is the notable feature in the first stage while the unity and low ratio are the observable marks for the second and third phases. The specifics of each phase are reviewed in the following:

1) **Phase 1: diversification phase (high-velocity ratio)** This stage devotions for finding the search space (exploration stage) therefore it is performed for the first third of the total number of development (i.e., $\frac{1}{3}t_{max}$). In this stage the prey moves very fast searching for its food meanwhile the predator stands without moving. Faramarzi *et al.* [45] modeled this stage based on the following formula:

$$S_i = R_B \bigotimes (Elite_i - R_B \bigotimes Z_i), \ i = 1, 2, \ldots, n \tag{11}$$

$$Z_i = Z_i + P.R \bigotimes S_i \tag{12}$$

where, $R \in [0, 1]$ and $P = 0.5$ serve as a vector of uniform random numbers and a constant number, respectively. $R_B$ is a random vector that refers to the brownian motion. $\bigotimes$ indicates the process of element-wise multiplications.

2) **Phase 2: Unit velocity ratio** This phase is a transportable stage out of the diversification to intensification where both prey and predator action with practically identical velocity looking for the foods of theirs. This phase is the center stage of the algorithm and it is implemented when $\frac{1}{3}t_{max} < t < \frac{2}{3}t_{max}$. In this case, the best tactic for the predator to follow brownian while the prey to move with lévy flight. For this particular phase Faramarzi *et al.* [45] divided the population for 2 halves and applied Eqs. (13)-(14) to emulate the activity of the first one half of the population and Eq. (18)-(19) for the $2^{nd}$ half as outlined below.

$$S_i = R_L \bigotimes (Elite_i - R_L \bigotimes Z_i), \ i = 1, 2, \ldots, n \tag{13}$$

$$Z_i = Z_i + P.R \bigotimes S_i \tag{14}$$

where, $R_L$ represents the random numbers follows Lévy distribution. Eq. (13)-(14) are applied to the first half of the population that represents the exploitation. While for the second half of the population follows the following equations.

$$S_i = R_B \bigotimes (R_B \bigotimes Elite_i - Z_i), \ i = 1, 2, \ldots, n \tag{15}$$

$$Z_i = Elite_i + P.CF \bigotimes S_i, \tag{16}$$

$$CF = (1 - \frac{t}{t_{max}})^{2\frac{t}{t_{max}}} \tag{17}$$

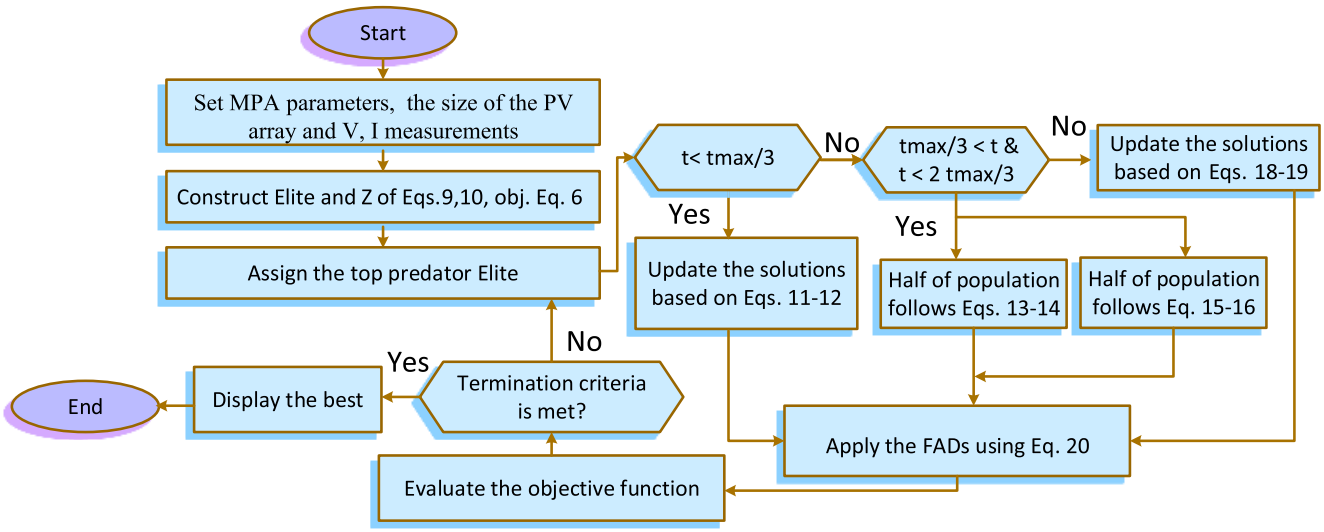


**FIGURE 4.** Flowchart of MPA technique.

where, $CF$ is parameter that controls the step size of movement for predator.

3) **Phase 3: Intensification (low-velocity ratio)** This stage may be the last phase in the search process. In this phase, the predator moves faster than the prey that is why it follows Lévy during updates its position. This stage executed on the last third of the iteration amounts ($t > \frac{2}{3}t_{max}$) which defined as:

$$S_i = R_L \bigotimes (R_L \bigotimes Elite_i - Z_i), \quad i = 1, 2, \ldots, n \tag{18}$$

$$Z_i = Elite_i + P.CF \bigotimes S_i, \quad CF = (1 - \frac{t}{t_{max}})^{2\frac{t}{t_{max}}} \tag{19}$$

4) **Eddy development and fish aggregating devices' outcome (FADS)** The surrounded environment has a huge effect on the act of the creature, thus Faramarzi *et al.* [45] considered the external impacts from the environment such as the eddy formation or fish aggregating devices (FADs) effects to avoid trapping the MPA in the local optimum solutions. The mathematical formula for this stage can be modeled as below:

$$Z_i = \begin{cases} Z_i + CF[Z_{min} + R \bigotimes (Z_{max} - Z_{min})] \bigotimes U \\ r_5 < FAD \\ Z_i + [FAD(1-r) + r](Z_{r1} - Z_{r2}) \\ r_5 > FAD \end{cases} \tag{20}$$

In Eq. (20), $FAD = 0.2$, and $U$ is a binary option and this is performed by creating arbitrary solution and then converted it into binary consuming threshold 0.2. $r \in [0, 1]$ symbolizes an arbitrary number. $r_1$ and $r_2$ is the list of the prey.

5) **Marine memory** Marine predators have a powerful memory of the place in which they have been effective in foraging. This particular function is applied by saving the optimal solutions in each iteration. The saved solutions are updated upon better solutions are identified.

The flowchart of the MPA algorithm is depicted in Fig. 4 to summarize the structure of the proposed algorithm.

## VI. SIMULATIONS AND RESULTS

The framework of this section is divided into two stages;

1) The first one is a comparison among the results provided by merging the weighted objective function as well as the novel one with the proposed algorithms. It is presented to clarify the applicability of the proposed objective function and its impact on the algorithms. For fair comparison in this part, both of PSO and HHO are implemented on the novel objective function to be able to compare their results with the published ones based on the weighted objective function published in the manuscripts of Babu *et al.* [10] and Yousri *et al.* [38].
2) Secondly, a comparison among the algorithms is performed to determine the best algorithm for the PV reconfiguration approach and the results are verified through several analyses.

The proposed algorithms are implemented with population size and iterations of 20, and 100, respectively for 30 independent runs. All the simulations and analyses are implemented and computed on "MATLAB 2018" platform on a laptop with Core i7-6500U CPU, 2.5 GHz of speed and 4 GB of RAM. The electric specification of the considered PV module of the arrays are as follow: open circuit Voltage ($V_{ocn}$) is 44.2 (V), and short circuit current ($I_{sc}$) is 5.2 (A). Temperature Coefficients: $K_v = -0.39851 \times V_{ocn}$ and $K_i = 0.015 \times I_{sc}$.

### A. COMPARISON BETWEEN THE NOVEL OBJECTIVE FUNCTION AND THE WEIGHTED OBJECTIVE FUNCTION IN LITERATURE

In this section, a comparison between the results of the algorithms based on the weighted objective function and the novel objective function of Eq. 6 is performed to evaluate the influence of the novel objective function on the algorithms performance. Therefore, two shade patterns of $9 \times 9$ PV array are studied. The shade patterns are classified as follows:

1) Pattern 1: short broad shading where the surface of the PV array is subjected to five levels of sun illumination which are equal 900 $W/m^2$, 800 $W/m^2$, 600 $W/m^2$, 400 $W/m^2$, and 200 $W/m^2$.
2) Pattern 2: long broad shading where the first six columns in the array receive 900 $W/m^2$ and the others are subjected to 800 $W/m^2$, 700 $W/m^2$, 400 $W/m^2$, and 300 $W/m^2$.

The shaded PV array in a TCT arrangement and the obtained reconfigured structure by MPA, MRFO, PSO, and HHO based on weighted objective function and the novel one are depicted in Figs. 5(a), 5(b) and 6(a), 6(b) for pattern 1 and 2, respectively. The corresponded current, voltage and power values for the exhibited patterns are calculated in Tables 1 and 2 for pattern 1 and 2, respectively.

The following lines clarify the methodology of calculating the rows current, voltage and power for pattern 1 of Figs. 5(a) and 5(b).

- The calculation of row currents for the TCT scheme can be given as follows:
  - For the first 5 rows, the currents have the same value, which are computed as shown: $I_{R1}$ to $I_{R5} = 9\left(\frac{900}{1000}\right)I_M = 8.1\, I_M$.
  - Row currents for $6^{th}$ row can be given as follows: $I_{R6} = 9\left(\frac{800}{1000}\right)I_M = 7.2\, I_M$.
  - Row currents for rows 7, 8, and 9 can be given as follows: $I_{R7} = I_{R8} = I_{R9} = 3\left(\frac{600}{1000}\right)I_M + 3\left(\frac{400}{1000}\right)I_M + 3\left(\frac{200}{1000}\right)I_M = 3.6\, I_M$.
- The calculation of row currents for the PSO method based on weighted objective function as in Fig. 5(a) can be given as follows:
  - The row current for the $1^{st}$ row can be calculated as $I_{R1} = 5\left(\frac{900}{1000}\right)I_M + 1\left(\frac{800}{1000}\right)I_M + 2\left(\frac{600}{1000}\right)I_M + 1\left(\frac{200}{1000}\right)I_M = 6.7\, I_M$.
  - The row current for the $2^{nd}$ row can be calculated as $I_{R2} = 4\left(\frac{900}{1000}\right)I_M + 1\left(\frac{800}{1000}\right)I_M + 2\left(\frac{600}{1000}\right)I_M + 1\left(\frac{400}{1000}\right)I_M + 1\left(\frac{200}{1000}\right)I_M = 6.2\, I_M$.
  - The row current for the $3^{rd}$ row can be calculated as $I_{R3} = 5\left(\frac{900}{1000}\right)I_M + 1\left(\frac{800}{1000}\right)I_M + 1\left(\frac{600}{1000}\right)I_M + 1\left(\frac{400}{1000}\right)I_M + 1\left(\frac{200}{1000}\right)I_M = 6.5\, I_M$.
  - The row current for the $4^{th}$ row can be calculated as $I_{R4} = 5\left(\frac{900}{1000}\right)I_M + 1\left(\frac{800}{1000}\right)I_M + 2\left(\frac{400}{1000}\right)I_M + 1\left(\frac{200}{1000}\right)I_M = 6.3\, I_M$.
  - The row current for the $5^{th}$ row can be calculated as $I_{R5} = 4\left(\frac{900}{1000}\right)I_M + 2\left(\frac{800}{1000}\right)I_M + 1\left(\frac{600}{1000}\right)I_M + 1\left(\frac{400}{1000}\right)I_M + 1\left(\frac{200}{1000}\right)I_M = 6.4\, I_M$.
  - The row current for the $6^{th}$ row can be calculated as $I_{R6} = 5\left(\frac{900}{1000}\right)I_M + 2\left(\frac{800}{1000}\right)I_M + 2\left(\frac{400}{1000}\right)I_M = 6.9\, I_M$.
  - The row current for the $7^{th}$ row can be calculated as $I_{R7} = 6\left(\frac{900}{1000}\right)I_M + 1\left(\frac{600}{1000}\right)I_M + 2\left(\frac{200}{1000}\right)I_M = 6.4\, I_M$.
  - The row current for the $8^{th}$ row can be calculated as $I_{R8} = 5\left(\frac{900}{1000}\right)I_M + 1\left(\frac{800}{1000}\right)I_M + 1\left(\frac{600}{1000}\right)I_M + 2\left(\frac{400}{1000}\right)I_M = 6.7\, I_M$.
  - The row current for the $9^{th}$ row can be calculated as $I_{R9} = 6\left(\frac{900}{1000}\right)I_M + 1\left(\frac{600}{1000}\right)I_M + 2\left(\frac{200}{1000}\right)I_M = 6.4\, I_M$.
- The calculation of row currents for the PSO method based on novel objective function as in Fig. 5(b)can be given as follows:
  - The row current for the $1^{st}$ row can be calculated as $I_{R1} = 7\left(\frac{900}{1000}\right)I_M + 1\left(\frac{600}{1000}\right)I_M + 1\left(\frac{200}{1000}\right)I_M = 7.1\, I_M$.
  - The row current for the $2^{nd}$ row can be calculated as $I_{R2} = 4\left(\frac{900}{1000}\right)I_M + 1\left(\frac{800}{1000}\right)I_M + 2\left(\frac{600}{1000}\right)I_M + 2\left(\frac{400}{1000}\right)I_M = 6.4\, I_M$.
  - The row current for the $3^{rd}$ row can be calculated as $I_{R3} = 5\left(\frac{900}{1000}\right)I_M + 2\left(\frac{600}{1000}\right)I_M + 1\left(\frac{400}{1000}\right)I_M + 1\left(\frac{200}{1000}\right)I_M = 6.3\, I_M$.
  - The row current for the $4^{th}$ row can be calculated as $I_{R4} = 5\left(\frac{900}{1000}\right)I_M + 1\left(\frac{800}{1000}\right)I_M + 2\left(\frac{400}{1000}\right)I_M + 1\left(\frac{200}{1000}\right)I_M = 6.3\, I_M$.
  - The row current for the $5^{th}$ row can be calculated as $I_{R5} = 4\left(\frac{900}{1000}\right)I_M + 1\left(\frac{800}{1000}\right)I_M + 2\left(\frac{600}{1000}\right)I_M + 2\left(\frac{400}{1000}\right)I_M = 6.4\, I_M$.
  - The row current for the $6^{th}$ row can be calculated as $I_{R6} = 7\left(\frac{900}{1000}\right)I_M + 2\left(\frac{200}{1000}\right)I_M = 6.7\, I_M$.
  - The row current for the $7^{th}$ row can be calculated as $I_{R7} = 4\left(\frac{900}{1000}\right)I_M + 3\left(\frac{800}{1000}\right)I_M + 1\left(\frac{400}{1000}\right)I_M + 1\left(\frac{200}{1000}\right)I_M = 6.6\, I_M$.
  - The row current for the $8^{th}$ row can be calculated as $I_{R8} = 5\left(\frac{900}{1000}\right)I_M + 1\left(\frac{800}{1000}\right)I_M + 1\left(\frac{600}{1000}\right)I_M + 2\left(\frac{200}{1000}\right)I_M = 6.3\, I_M$.

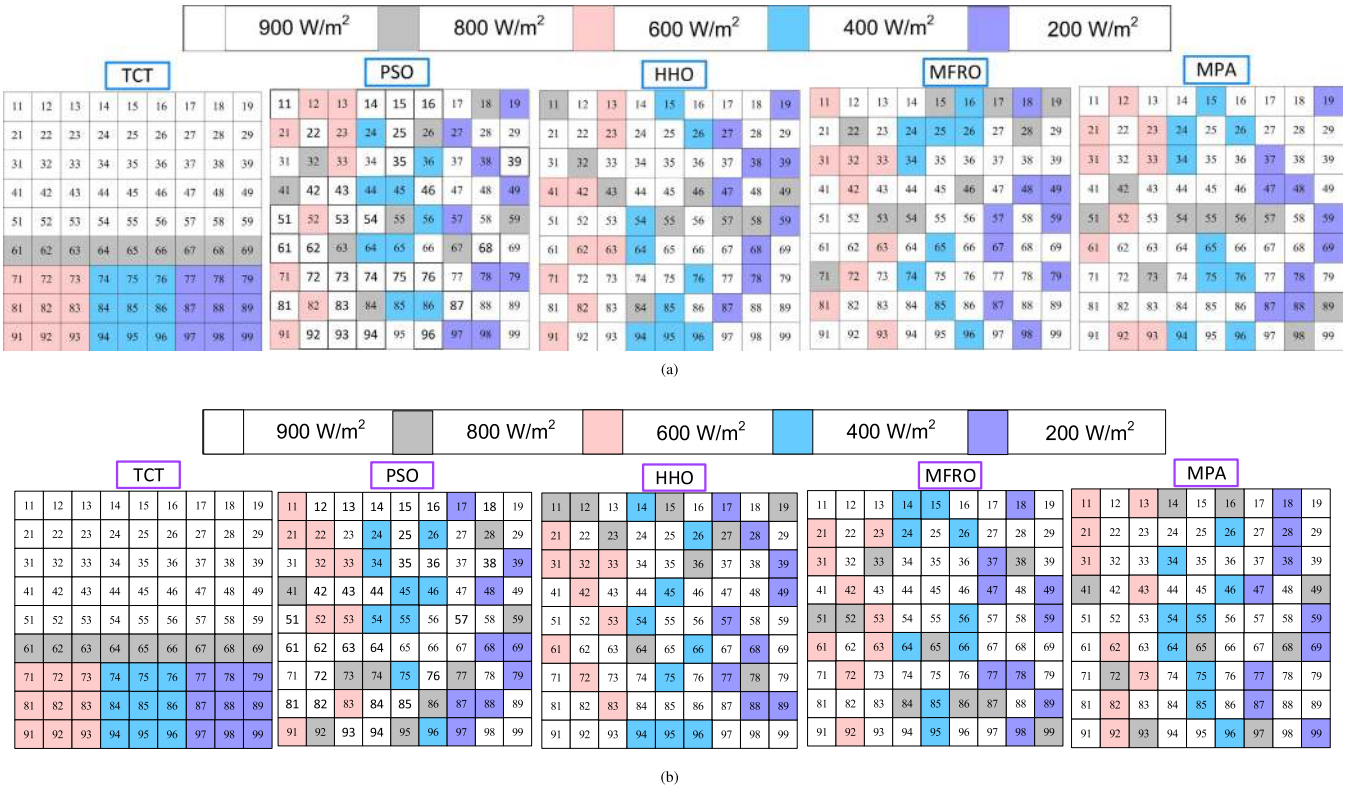


**FIGURE 5.** Dispersion of shade by employing proposed algorithms based on (a) weighted objective function, and (b) novel objective function for pattern 1.

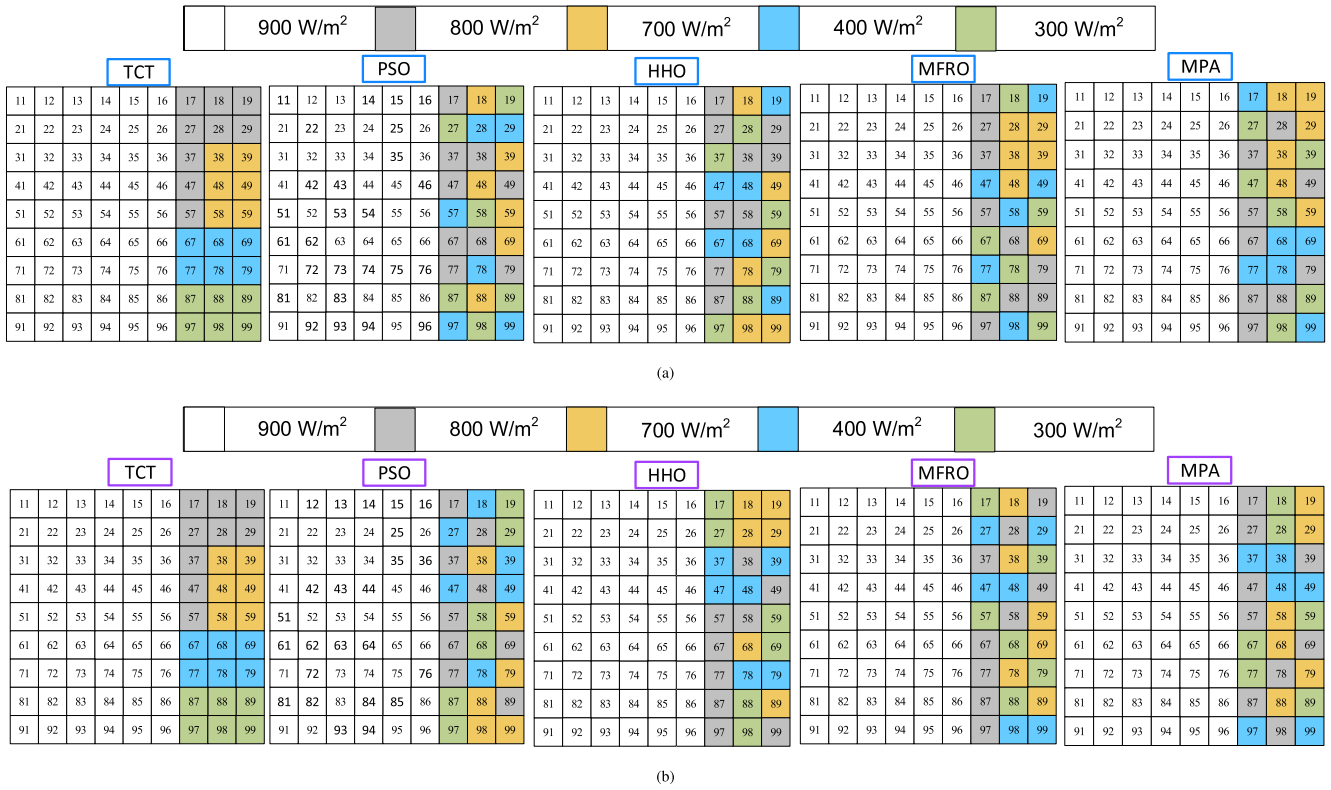


**FIGURE 6.** Dispersion of shade by employing proposed algorithms based on (a) weighted objective function, and (b) novel objective function for pattern 2.

  - The row current for the $9^{th}$ row can be calculated as $I_{R9} = 4\left(\frac{900}{1000}\right)I_M + 2\left(\frac{800}{1000}\right)I_M + 1\left(\frac{600}{1000}\right)I_M + 1\left(\frac{400}{1000}\right)I_M + 1\left(\frac{200}{1000}\right)I_M = 6.4\, I_M$.
- The calculation of row currents for the MPA method based on weighted objective function as in Fig. 5(a) can be given as follows:
  - The row current for the $1^{st}$ row can be calculated as $I_{R1} = 6\left(\frac{900}{1000}\right)I_M + 1\left(\frac{600}{1000}\right)I_M + 1\left(\frac{400}{1000}\right)I_M + 1\left(\frac{200}{1000}\right)I_M = 6.6\, I_M$.
  - The row current for the $2^{nd}$ row can be calculated as $I_{R2} = 5\left(\frac{900}{1000}\right)I_M + 2\left(\frac{600}{1000}\right)I_M + 2\left(\frac{400}{1000}\right)I_M = 6.5\, I_M$.
  - The row current for the $3^{rd}$ row can be calculated as $I_{R3} = 5\left(\frac{900}{1000}\right)I_M + 2\left(\frac{600}{1000}\right)I_M + 1\left(\frac{400}{1000}\right)I_M + 1\left(\frac{200}{1000}\right)I_M = 6.3\, I_M$.
  - The row current for the $4^{th}$ row can be calculated as $I_{R4} = 6\left(\frac{900}{1000}\right)I_M + 1\left(\frac{800}{1000}\right)I_M + 2\left(\frac{200}{1000}\right)I_M = 6.6\, I_M$.
  - The row current for the $5^{th}$ row can be calculated as $I_{R5} = 2\left(\frac{900}{1000}\right)I_M + 5\left(\frac{800}{1000}\right)I_M + 1\left(\frac{600}{1000}\right)I_M + 1\left(\frac{200}{1000}\right)I_M = 6.6\, I_M$.
  - The row current for the $6^{th}$ row can be calculated as $I_{R6} = 6\left(\frac{900}{1000}\right)I_M + 1\left(\frac{600}{1000}\right)I_M + 1\left(\frac{400}{1000}\right)I_M + 1\left(\frac{200}{1000}\right)I_M = 6.6\, I_M$.
  - The row current for the $7^{th}$ row can be calculated as $I_{R7} = 5\left(\frac{900}{1000}\right)I_M + 1\left(\frac{800}{1000}\right)I_M + 2\left(\frac{400}{1000}\right)I_M + 1\left(\frac{200}{1000}\right)I_M = 6.3\, I_M$.
  - The row current for the $8^{th}$ row can be calculated as $I_{R8} = 6\left(\frac{900}{1000}\right)I_M + 1\left(\frac{800}{1000}\right)I_M + 2\left(\frac{200}{1000}\right)I_M = 6.6\, I_M$.
  - The row current for the $9^{th}$ row can be calculated as $I_{R9} = 4\left(\frac{900}{1000}\right)I_M + 1\left(\frac{800}{1000}\right)I_M + 2\left(\frac{600}{1000}\right)I_M + 2\left(\frac{400}{1000}\right)I_M = 6.4\, I_M$.
- The calculation of row currents for the MPA method based on novel objective function as in Fig. 5(b) can be given as follows:
  - The row current for the $1^{st}$ row can be calculated as $I_{R1} = 4\left(\frac{900}{1000}\right)I_M + 2\left(\frac{800}{1000}\right)I_M + 2\left(\frac{600}{1000}\right)I_M + 1\left(\frac{200}{1000}\right)I_M = 6.6\, I_M$.
  - The row current for the $2^{nd}$ row can be calculated as $I_{R2} = 6\left(\frac{900}{1000}\right)I_M + 1\left(\frac{600}{1000}\right)I_M + 1\left(\frac{400}{1000}\right)I_M + 1\left(\frac{200}{1000}\right)I_M = 6.6\, I_M$.
  - The row current for the $3^{rd}$ row can be calculated as $I_{R3} = 6\left(\frac{900}{1000}\right)I_M + 1\left(\frac{600}{1000}\right)I_M + 1\left(\frac{400}{1000}\right)I_M + 1\left(\frac{200}{1000}\right)I_M = 6.6\, I_M$.
  - The row current for the $4^{th}$ row can be calculated as $I_{R4} = 4\left(\frac{900}{1000}\right)I_M + 2\left(\frac{800}{1000}\right)I_M + 1\left(\frac{600}{1000}\right)I_M + 1\left(\frac{400}{1000}\right)I_M + 1\left(\frac{200}{1000}\right)I_M = 6.4\, I_M$.
  - The row current for the $5^{th}$ row can be calculated as $I_{R5} = 6\left(\frac{900}{1000}\right)I_M + 2\left(\frac{400}{1000}\right)I_M + 1\left(\frac{200}{1000}\right)I_M = 6.4\, I_M$.
  - The row current for the $6^{th}$ row can be calculated as $I_{R6} = 4\left(\frac{900}{1000}\right)I_M + 2\left(\frac{800}{1000}\right)I_M + 1\left(\frac{600}{1000}\right)I_M + 1\left(\frac{400}{1000}\right)I_M + 1\left(\frac{200}{1000}\right)I_M = 6.4\, I_M$.
  - The row current for the $7^{th}$ row can be calculated as $I_{R7} = 5\left(\frac{900}{1000}\right)I_M + 1\left(\frac{800}{1000}\right)I_M + 1\left(\frac{600}{1000}\right)I_M + 1\left(\frac{400}{1000}\right)I_M + 1\left(\frac{200}{1000}\right)I_M = 6.5\, I_M$.
  - The row current for the $8^{th}$ row can be calculated as $I_{R8} = 6\left(\frac{900}{1000}\right)I_M + 1\left(\frac{600}{1000}\right)I_M + 1\left(\frac{400}{1000}\right)I_M + 1\left(\frac{200}{1000}\right)I_M = 6.6\, I_M$.
  - The row current for the $9^{th}$ row can be calculated as $I_{R9} = 4\left(\frac{900}{1000}\right)I_M + 2\left(\frac{800}{1000}\right)I_M + 1\left(\frac{600}{1000}\right)I_M + 1\left(\frac{400}{1000}\right)I_M + 1\left(\frac{200}{1000}\right)I_M = 6.4\, I_M$.

By following the above procedure the row current values for the other two methods (HHO, MFRO) are calculated and presented in Table 1. Similarly, rows current values for pattern 2 also calculated and listed in Table 2.

The listed power values show that the algorithms based on the novel objective function achieves higher harvested power from the considered array for the two shaded patterns. The PSO based on the weighted objective function provides 55.8 $V_M I_M$ for pattern 1 and 58.5 $V_M I_M$ for pattern 2 whilst it achieves power values of 56.7 $V_M I_M$ and 62.1 $V_M I_M$ in case of applying the novel objective function. Similarly, HHO, MRFO and MPA based on the novel objective function boost the values of the harvested PV power from 56.7 $V_M I_M$ and 62.1 $V_M I_M$ to 57.6 $V_M I_M$ and 63 $V_M I_M$ for the considered shadow patterns, respectively. Accordingly, employing the objective function of equation 6 enhances the performance of the optimization algorithms in discovering the search space efficiently. Therefore authors recommend it for the reconfiguration PV array optimization problem as not only the issues of selecting the values of the adequate weights in the weighted obj has been tackled but also it helped the algorithms to provide higher harvested power.

### B. COMPARISONS AMONG THE PROPOSED ALGORITHMS

From the previous subsection, the novel objective function confirms its remarkable impact on the algorithms performance as a higher harvested PV power values are obtained based on their corresponded patterns. In this part a comparison among the algorithms results based on the novel objective function is carried-out to demonstrate the best algorithm. In this part the P-V, I-V characteristics and mean execution time of the proposed algorithms are considered. Moreover, several quality measures, namely mismatch power loss, fill

**TABLE 1. Analysis of TCT, PSO, HHO, MPA and MRFA for 9 × 9 PV array shade pattern 1 in the Ref [36] based on the weighted objective function and the novel one.**

| Results based Weighted obj [38] [10] [16] | | | | | | | | | | | | | | | | | | | | |
|---|---|---|---|---|---|---|---|---|---|---|---|---|---|---|---|---|---|---|---|---|
| TCT scheme | | | | PSO scheme [36] | | | | HHO scheme [38] | | | | MRFO scheme | | | | MPA scheme | | | | |
| $I_{Ri}$ | $I_R(A)$ | $V_m(V)$ | $P(W)$ | $I_{Ri}$ | $I_R(A)$ | $V_m(V)$ | $P(W)$ | $I_{Ri}$ | $I_R(A)$ | $V_m(V)$ | $P(W)$ | $I_{Ri}$ | $I_R(A)$ | $V_m(V)$ | $P(W)$ | $I_{Ri}$ | $I_R(A)$ | $V_m(V)$ | $P(W)$ | |
| $I_{R7}$ | $3.6I_M$ | $9V_M$ | $32.4V_MI_M$ | $I_{R2}$ | $6.2I_M$ | $9V_M$ | $55.8V_MI_M$ | $I_{R6}$ | $6.3I_M$ | $9V_M$ | $56.7V_MI_M$ | $I_{R1}$ | $6.3\,I_m$ | $9\,V_m$ | $56.7\,I_mV_m$ | $I_{R3}$ | $6.3\,I_m$ | $9\,V_m$ | $56.7\,I_mV_m$ | |
| $I_{R8}$ | $3.6I_M$ | $9V_M$ | $32.4V_MI_M$ | $I_{R4}$ | $6.3I_M$ | $8V_M$ | $50.4V_MI_M$ | $I_{R9}$ | $6.3I_M$ | $9V_M$ | $56.7V_MI_M$ | $I_{R4}$ | $6.3\,I_m$ | $9\,V_m$ | $56.7\,I_mV_m$ | $I_{R7}$ | $6.3\,I_m$ | $9\,V_m$ | $56.7\,I_mV_m$ | |
| $I_{R9}$ | $3.6I_M$ | $9V_M$ | $32.4V_MI_M$ | $I_{R5}$ | $6.4I_M$ | $7V_M$ | $44.8V_MI_M$ | $I_{R1}$ | $6.5I_M$ | $7V_M$ | $45.5V_MI_M$ | $I_{R2}$ | $6.4\,I_m$ | $7\,V_m$ | $44.8\,I_mV_m$ | $I_{R9}$ | $6.4\,I_m$ | $7\,V_m$ | $44.8\,I_mV_m$ | |
| $I_{R6}$ | $7.2I_M$ | $6V_M$ | $43.2V_MI_M$ | $I_{R7}$ | $6.4I_M$ | $7V_M$ | $44.8V_MI_M$ | $I_{R4}$ | $6.5I_M$ | $7V_M$ | $45.5V_MI_M$ | $I_{R5}$ | $6.5\,I_m$ | $6\,V_m$ | $39\,I_mV_m$ | $I_{R2}$ | $6.5\,I_m$ | $6\,V_m$ | $39\,I_mV_m$ | |
| $I_{R5}$ | $8.1I_M$ | $5V_M$ | $40.5V_MI_M$ | $I_{R9}$ | $6.4I_M$ | $7V_M$ | $44.8V_MI_M$ | $I_{R8}$ | $6.5I_M$ | $7V_M$ | $45.5V_MI_M$ | $I_{R7}$ | $6.5\,I_m$ | $6\,V_m$ | $39\,I_mV_m$ | $I_{R1}$ | $6.6\,I_m$ | $5\,V_m$ | $33\,I_mV_m$ | |
| $I_{R4}$ | $8.1I_M$ | $5V_M$ | $40.5V_MI_M$ | $I_{R3}$ | $6.5I_M$ | $4V_M$ | $26V_MI_M$ | $I_{R2}$ | $6.6I_M$ | $4V_M$ | $26.4V_MI_M$ | $I_{R6}$ | $6.6\,I_m$ | $4\,V_m$ | $26.4\,I_mV_m$ | $I_{R4}$ | $6.6\,I_m$ | $5\,V_m$ | $33\,I_mV_m$ | |
| $I_{R3}$ | $8.1I_M$ | $5V_M$ | $40.5V_MI_M$ | $I_{R1}$ | $6.7I_M$ | $3V_M$ | $20.1V_MI_M$ | $I_{R3}$ | $6.6I_M$ | $4V_M$ | $26.4V_MI_M$ | $I_{R8}$ | $6.6\,I_m$ | $4\,V_m$ | $26.4\,I_mV_m$ | $I_{R5}$ | $6.6\,I_m$ | $5\,V_m$ | $33\,I_mV_m$ | |
| $I_{R2}$ | $8.1I_M$ | $5V_M$ | $40.5V_MI_M$ | $I_{R8}$ | $6.7I_M$ | $3V_M$ | $20.1V_MI_M$ | $I_{R5}$ | $6.6I_M$ | $4V_M$ | $26.4V_MI_M$ | $I_{R9}$ | $6.6\,I_m$ | $4\,V_m$ | $26.4\,I_mV_m$ | $I_{R6}$ | $6.6\,I_m$ | $5\,V_m$ | $33\,I_mV_m$ | |
| $I_{R1}$ | $8.1I_M$ | $5V_M$ | $40.5V_MI_M$ | $I_{R6}$ | $6.9I_M$ | $1V_M$ | $6.9V_MI_M$ | $I_{R7}$ | $6.6I_M$ | $4V_M$ | $26.4V_MI_M$ | $I_{R3}$ | $6.7\,I_m$ | $1\,V_m$ | $6.7\,I_mV_m$ | $I_{R8}$ | $6.6\,I_m$ | $5\,V_m$ | $33\,I_mV_m$ | |
| Results based novel objective function, Eq. 6 | | | | | | | | | | | | | | | | | | | | |
| TCT scheme | | | | PSO scheme | | | | HHO scheme | | | | MRFO scheme | | | | MPA scheme | | | | |
| $I_{Ri}$ | $I_R(A)$ | $V_m(V)$ | $P(W)$ | $I_{Ri}$ | $I_R(A)$ | $V_m(V)$ | $P(W)$ | $I_{Ri}$ | $I_R(A)$ | $V_m(V)$ | $P(W)$ | $I_{Ri}$ | $I_R(A)$ | $V_m(V)$ | $P(W)$ | $I_{Ri}$ | $I_R(A)$ | $V_m(V)$ | $P(W)$ | |
| $I_{R7}$ | $3.6\,I_M$ | $9\,V_M$ | $32.4\,I_MV_M$ | $I_{R3}$ | $6.3\,I_M$ | $9\,V_M$ | $56.7\,I_MV_M$ | $I_{R2}$ | $6.4\,I_M$ | $9\,V_M$ | $57.6\,I_MV_M$ | $I_{R1}$ | $6.4\,I_M$ | $9\,V_M$ | $57.6\,I_MV_M$ | $I_{R4}$ | $6.4\,I_M$ | $9\,V_M$ | $57.6\,I_MV_M$ | |
| $I_{R8}$ | $3.6\,I_M$ | $9\,V_M$ | $32.4\,I_MV_M$ | $I_{R4}$ | $6.3\,I_M$ | $9\,V_M$ | $56.7\,I_MV_M$ | $I_{R3}$ | $6.4\,I_M$ | $9\,V_M$ | $57.6\,I_MV_M$ | $I_{R4}$ | $6.4\,I_M$ | $9\,V_M$ | $57.6\,I_MV_M$ | $I_{R5}$ | $6.4\,I_M$ | $9\,V_M$ | $57.6\,I_MV_M$ | |
| $I_{R9}$ | $3.6\,I_M$ | $9\,V_M$ | $32.4\,I_MV_M$ | $I_{R8}$ | $6.3\,I_M$ | $9\,V_M$ | $56.7\,I_MV_M$ | $I_{R8}$ | $6.4\,I_M$ | $9\,V_M$ | $57.6\,I_MV_M$ | $I_{R5}$ | $6.4\,I_M$ | $9\,V_M$ | $57.6\,I_MV_M$ | $I_{R6}$ | $6.4\,I_M$ | $9\,V_M$ | $57.6\,I_MV_M$ | |
| $I_{R6}$ | $7.2\,I_M$ | $6\,V_M$ | $43.2\,I_MV_M$ | $I_{R2}$ | $6.4\,I_M$ | $6\,V_M$ | $38.4\,I_MV_M$ | $I_{R1}$ | $6.5\,I_M$ | $6\,V_M$ | $39\,I_MV_M$ | $I_{R6}$ | $6.4\,I_M$ | $9\,V_M$ | $57.6\,I_MV_M$ | $I_{R9}$ | $6.4\,I_M$ | $9\,V_M$ | $57.6\,I_MV_M$ | |
| $I_{R1}$ | $8.1\,I_M$ | $5\,V_M$ | $40.5\,I_MV_M$ | $I_{R5}$ | $6.4\,I_M$ | $6\,V_M$ | $38.4\,I_MV_M$ | $I_{R6}$ | $6.5\,I_M$ | $6\,V_M$ | $39\,I_MV_M$ | $I_{R7}$ | $6.4\,I_M$ | $9\,V_M$ | $57.6\,I_MV_M$ | $I_{R7}$ | $6.5\,I_M$ | $5\,V_M$ | $32.5\,I_MV_M$ | |
| $I_{R2}$ | $8.1\,I_M$ | $5\,V_M$ | $40.5\,I_MV_M$ | $I_{R9}$ | $6.4\,I_M$ | $6\,V_M$ | $38.4\,I_MV_M$ | $I_{R7}$ | $6.5\,I_M$ | $6\,V_M$ | $39\,I_MV_M$ | $I_{R2}$ | $6.5\,I_M$ | $4\,V_M$ | $26\,I_MV_M$ | $I_{R1}$ | $6.6\,I_M$ | $4\,V_M$ | $26.4\,I_MV_M$ | |
| $I_{R3}$ | $8.1\,I_M$ | $5\,V_M$ | $40.5\,I_MV_M$ | $I_{R7}$ | $6.6\,I_M$ | $3\,V_M$ | $19.8\,I_MV_M$ | $I_{R4}$ | $6.6\,I_M$ | $3\,V_M$ | $19.8\,I_MV_M$ | $I_{R9}$ | $6.5\,I_M$ | $4\,V_M$ | $26\,I_MV_M$ | $I_{R2}$ | $6.6\,I_M$ | $4\,V_M$ | $26.4\,I_MV_M$ | |
| $I_{R4}$ | $8.1\,I_M$ | $5\,V_M$ | $40.5\,I_MV_M$ | $I_{R6}$ | $6.7\,I_M$ | $2\,V_M$ | $13.4\,I_MV_M$ | $I_{R5}$ | $6.6\,I_M$ | $3\,V_M$ | $19.8\,I_MV_M$ | $I_{R8}$ | $6.6\,I_M$ | $2\,V_M$ | $13.2\,I_MV_M$ | $I_{R3}$ | $6.6\,I_M$ | $4\,V_M$ | $26.4\,I_MV_M$ | |
| $I_{R5}$ | $8.1\,I_M$ | $5\,V_M$ | $40.5\,I_MV_M$ | $I_{R1}$ | $7.1\,I_M$ | $1\,V_M$ | $7.1\,I_MV_M$ | $I_{R9}$ | $6.6\,I_M$ | $3\,V_M$ | $19.8\,I_MV_M$ | $I_{R3}$ | $6.9\,I_M$ | $1\,V_M$ | $6.9\,I_MV_M$ | $I_{R8}$ | $6.6\,I_M$ | $4\,V_M$ | $26.4\,I_MV_M$ | |

**TABLE 2. Analysis of TCT, PSO, HHO, MPA and MRFA for 9 × 9 PV array shade pattern 2 in the Ref [36] based on the weighted objective function and the novel one.**

| Results based Weighted obj [38] [10] [16] | | | | | | | | | | | | | | | | | | | | |
|---|---|---|---|---|---|---|---|---|---|---|---|---|---|---|---|---|---|---|---|---|
| TCT scheme | | | | PSO scheme [36] | | | | HHO scheme [38] | | | | MRFO scheme | | | | MPA scheme | | | | |
| $I_{Ri}$ | $I_R(A)$ | $V_m(V)$ | $P(W)$ | $I_{Ri}$ | $I_R(A)$ | $V_m(V)$ | $P(W)$ | $I_{Ri}$ | $I_R(A)$ | $V_m(V)$ | $P(W)$ | $I_{Ri}$ | $I_R(A)$ | $V_m(V)$ | $P(W)$ | $I_{Ri}$ | $I_R(A)$ | $V_m(V)$ | $P(W)$ | |
| $I_{R8}$ | $6.3I_M$ | $9V_M$ | $56.7V_MI_M$ | $I_{R2}$ | $6.5I_M$ | $9V_M$ | $58.5V_MI_M$ | $I_{R4}$ | $6.9I_M$ | $9V_M$ | $62.1V_MI_M$ | $I_{R1}$ | $6.9\,I_M$ | $9\,V_M$ | $62.1\,I_MV_M$ | $I_{R9}$ | $6.9\,I_M$ | $9\,V_M$ | $62.1\,I_MV_M$ | |
| $I_{R9}$ | $6.3I_M$ | $9V_M$ | $56.7V_MI_M$ | $I_{R9}$ | $6.5I_M$ | $9V_M$ | $58.5V_MI_M$ | $I_{R6}$ | $6.9I_M$ | $9V_M$ | $62.1V_MI_M$ | $I_{R4}$ | $6.9\,I_M$ | $9\,V_M$ | $62.1\,I_MV_M$ | $I_{R6}$ | $7\,I_M$ | $8\,V_M$ | $56\,I_MV_M$ | |
| $I_{R6}$ | $6.6I_M$ | $7V_M$ | $46.2V_MI_M$ | $I_{R8}$ | $6.7I_M$ | $7V_M$ | $46.9V_MI_M$ | $I_{R8}$ | $6.9I_M$ | $9V_M$ | $62.1V_MI_M$ | $I_{R5}$ | $6.9\,I_M$ | $9\,V_M$ | $62.1\,I_MV_M$ | $I_{R7}$ | $7\,I_M$ | $8\,V_M$ | $56\,I_MV_M$ | |
| $I_{R7}$ | $6.6I_M$ | $7V_M$ | $46.2V_MI_M$ | $I_{R5}$ | $6.8I_M$ | $6V_M$ | $40.8V_MI_M$ | $I_{R9}$ | $7.1I_M$ | $6V_M$ | $42.6V_MI_M$ | $I_{R7}$ | $6.9\,I_M$ | $9\,V_M$ | $62.1\,I_MV_M$ | $I_{R1}$ | $7.2\,I_M$ | $6\,V_M$ | $43.2\,I_MV_M$ | |
| $I_{R5}$ | $7.6I_M$ | $5V_M$ | $38V_MI_M$ | $I_{R1}$ | $7.2I_M$ | $5V_M$ | $36V_MI_M$ | $I_{R7}$ | $7.2I_M$ | $5V_M$ | $36V_MI_M$ | $I_{R9}$ | $6.9\,I_M$ | $9\,V_M$ | $62.1\,I_MV_M$ | $I_{R2}$ | $7.2\,I_M$ | $6\,V_M$ | $43.2\,I_MV_M$ | |
| $I_{R4}$ | $7.6I_M$ | $5V_M$ | $38V_MI_M$ | $I_{R7}$ | $7.4I_M$ | $4V_M$ | $29.6V_MI_M$ | $I_{R1}$ | $7.3I_M$ | $7V_M$ | $29.2V_MI_M$ | $I_{R6}$ | $7.2\,I_M$ | $4\,V_M$ | $28.8\,I_MV_M$ | $I_{R3}$ | $7.2\,I_M$ | $6\,V_M$ | $43.2\,I_MV_M$ | |
| $I_{R3}$ | $7.6I_M$ | $5V_M$ | $38V_MI_M$ | $I_{R3}$ | $7.7I_M$ | $3V_M$ | $23.1V_MI_M$ | $I_{R2}$ | $7.3I_M$ | $7V_M$ | $29.2V_MI_M$ | $I_{R8}$ | $7.3\,I_M$ | $3\,V_M$ | $21.9\,I_MV_M$ | $I_{R4}$ | $7.2\,I_M$ | $6\,V_M$ | $43.2\,I_MV_M$ | |
| $I_{R2}$ | $7.8I_M$ | $2V_M$ | $15.6V_MI_M$ | $I_{R4}$ | $7.7I_M$ | $3V_M$ | $23.1V_MI_M$ | $I_{R3}$ | $7.3I_M$ | $7V_M$ | $29.2V_MI_M$ | $I_{R2}$ | $7.6\,I_M$ | $2\,V_M$ | $15.2\,I_MV_M$ | $I_{R5}$ | $7.2\,I_M$ | $6\,V_M$ | $43.2\,I_MV_M$ | |
| $I_{R1}$ | $7.8I_M$ | $2V_M$ | $15.6V_MI_M$ | $I_{R6}$ | $7.7I_M$ | $3V_M$ | $23.1V_MI_M$ | $I_{R5}$ | $7.3I_M$ | $7V_M$ | $29.2V_MI_M$ | $I_{R3}$ | $7.6\,I_M$ | $2\,V_M$ | $15.2\,I_MV_M$ | $I_{R8}$ | $7.3\,I_M$ | $1\,V_M$ | $7.3\,I_MV_M$ | |
| Results based novel objective function, Eq. 6 | | | | | | | | | | | | | | | | | | | | |
| TCT scheme | | | | PSO scheme | | | | HHO scheme | | | | MRFO scheme | | | | MPA scheme | | | | |
| $I_{Ri}$ | $I_R(A)$ | $V_m(V)$ | $P(W)$ | $I_{Ri}$ | $I_R(A)$ | $V_m(V)$ | $P(W)$ | $I_{Ri}$ | $I_R(A)$ | $V_m(V)$ | $P(W)$ | $I_{Ri}$ | $I_R(A)$ | $V_m(V)$ | $P(W)$ | $I_{Ri}$ | $I_R(A)$ | $V_m(V)$ | $P(W)$ | |
| $I_{R8}$ | $6.3\,I_M$ | $9\,V_M$ | $56.7\,I_MV_M$ | $I_{R1}$ | $6.9\,I_M$ | $9\,V_M$ | $62.1\,I_MV_M$ | $I_{R3}$ | $7\,I_M$ | $9\,V_M$ | $63\,I_MV_M$ | $I_{R2}$ | $7\,I_M$ | $9\,V_M$ | $63\,I_MV_M$ | $I_{R3}$ | $7\,I_M$ | $9\,V_M$ | $63\,I_MV_M$ | |
| $I_{R9}$ | $6.3\,I_M$ | $9\,V_M$ | $56.7\,I_MV_M$ | $I_{R2}$ | $6.9\,I_M$ | $9\,V_M$ | $62.1\,I_MV_M$ | $I_{R4}$ | $7\,I_M$ | $9\,V_M$ | $63\,I_MV_M$ | $I_{R4}$ | $7\,I_M$ | $9\,V_M$ | $63\,I_MV_M$ | $I_{R4}$ | $7\,I_M$ | $9\,V_M$ | $63\,I_MV_M$ | |
| $I_{R6}$ | $6.6\,I_M$ | $7\,V_M$ | $46.2\,I_MV_M$ | $I_{R4}$ | $7\,I_M$ | $7\,V_M$ | $49\,I_MV_M$ | $I_{R7}$ | $7\,I_M$ | $9\,V_M$ | $63\,I_MV_M$ | $I_{R9}$ | $7\,I_M$ | $9\,V_M$ | $63\,I_MV_M$ | $I_{R9}$ | $7\,I_M$ | $9\,V_M$ | $63\,I_MV_M$ | |
| $I_{R7}$ | $6.6\,I_M$ | $7\,V_M$ | $46.2\,I_MV_M$ | $I_{R9}$ | $7.1\,I_M$ | $6\,V_M$ | $42.6\,I_MV_M$ | $I_{R1}$ | $7.1\,I_M$ | $6\,V_M$ | $42.6\,I_MV_M$ | $I_{R1}$ | $7.2\,I_M$ | $6\,V_M$ | $43.2\,I_MV_M$ | $I_{R1}$ | $7.2\,I_M$ | $6\,V_M$ | $43.2\,I_MV_M$ | |
| $I_{R3}$ | $7.6\,I_M$ | $5\,V_M$ | $38\,I_MV_M$ | $I_{R5}$ | $7.2\,I_M$ | $5\,V_M$ | $36\,I_MV_M$ | $I_{R2}$ | $7.1\,I_M$ | $6\,V_M$ | $42.6\,I_MV_M$ | $I_{R3}$ | $7.2\,I_M$ | $6\,V_M$ | $43.2\,I_MV_M$ | $I_{R2}$ | $7.2\,I_M$ | $6\,V_M$ | $43.2\,I_MV_M$ | |
| $I_{R4}$ | $7.6\,I_M$ | $5\,V_M$ | $38\,I_MV_M$ | $I_{R8}$ | $7.2\,I_M$ | $5\,V_M$ | $36\,I_MV_M$ | $I_{R6}$ | $7.2\,I_M$ | $4\,V_M$ | $28.8\,I_MV_M$ | $I_{R5}$ | $7.2\,I_M$ | $6\,V_M$ | $43.2\,I_MV_M$ | $I_{R5}$ | $7.2\,I_M$ | $6\,V_M$ | $43.2\,I_MV_M$ | |
| $I_{R5}$ | $7.6\,I_M$ | $5\,V_M$ | $38\,I_MV_M$ | $I_{R3}$ | $7.3\,I_M$ | $3\,V_M$ | $21.9\,I_MV_M$ | $I_{R8}$ | $7.2\,I_M$ | $4\,V_M$ | $28.8\,I_MV_M$ | $I_{R6}$ | $7.2\,I_M$ | $6\,V_M$ | $43.2\,I_MV_M$ | $I_{R6}$ | $7.2\,I_M$ | $6\,V_M$ | $43.2\,I_MV_M$ | |
| $I_{R1}$ | $7.8\,I_M$ | $2\,V_M$ | $15.6\,I_MV_M$ | $I_{R6}$ | $7.3\,I_M$ | $3\,V_M$ | $21.9\,I_MV_M$ | $I_{R5}$ | $7.3\,I_M$ | $2\,V_M$ | $14.6\,I_MV_M$ | $I_{R7}$ | $7.2\,I_M$ | $6\,V_M$ | $43.2\,I_MV_M$ | $I_{R7}$ | $7.2\,I_M$ | $6\,V_M$ | $43.2\,I_MV_M$ | |
| $I_{R2}$ | $7.8\,I_M$ | $2\,V_M$ | $15.6\,I_MV_M$ | $I_{R7}$ | $7.3\,I_M$ | $3\,V_M$ | $21.9\,I_MV_M$ | $I_{R9}$ | $7.3\,I_M$ | $2\,V_M$ | $14.6\,I_MV_M$ | $I_{R8}$ | $7.2\,I_M$ | $6\,V_M$ | $43.2\,I_MV_M$ | $I_{R8}$ | $7.2\,I_M$ | $6\,V_M$ | $43.2\,I_MV_M$ | |

factor, and percentage of power loss are taken into consideration. The mathematical formulas of the used factors can be written as follows:

- Mismatch power loss: $(P_{Mismatchloss}) = P_{Max_{IC}} - P_{GMPP_{PSC}}$
- Fill factor: $(FF) = \frac{(V_{mp}I_{mp})_{PSC}}{V_{OC}I_{SC}}$
- Percentage of power loss: $(\%P_{loss}) = \frac{GMPP_{STC} - GMPP_{PSC}}{GMPP_{STC}}$

Here, $IC$ is a fully irradiated condition. $P_{Max_{(IC)}}$ and $P_{GMPP_{(PSC)}}$ are the generated maximum power values during the fully irradiated condition and at PSC, respectively. $I_{mp}$ and $V_{mp}$ are the maximum produced values of current and voltage under the PSC, respectively. $I_{SC}$ and $V_{OC}$ represent the short circuit current and open circuit voltage, respectively. GMPP at STC and PSC are represented by $GMPP_{STC}$ and $GMPP_{PSC}$, respectively.

Figures 10 and 8 depicts several factors for comparing the proposed algorithms that included the accomplished I-V of Figs. 7(a)-7(b) and P-V characteristic's for the shade patterns of Figs. 5(b) and 6(b), respectively as well as the mismatched power loss of Figs.7(c)-8(c), the fill factor of Figs. 7(d)-8(d), the power loss values of Figs. 7(e)-8(e) and the mean execution time 7(f)-8(f) by the studied algorithms. The figures show that implementing the meta-heuristic algorithms for re-configuring the shaded arrays minimizes the mismatch power loss and tackle the multi-peak issue in the array characteristics. The MPA, MRFO and HHO based approach show the same response from the point of achieving maximum power value with regular distribution for the shadow. Hence, these approaches provide uni peak PV characteristics with highest fill factor values and lowest percentage power loss in comparison with PSO and TCT arrangements. Whereas MPA has the first rank in achieving the least mean execution time across the two studied patterns. Consequently, MPA is considered as the recommended one.

For validating the superiority of MPA statistically, the Wilcoxon signed rank test is computed to show a pairwise comparison among any two algorithms based on the following steps [46], [47];

1) Report the maximum power values over number of runs (30) for all the considered algorithms (MPA vs PSO, MPA vs HHO, and MPA vs MRFO).
2) Compute $R+$ that refers to the sum of ranks for runs in which MPA shows superiority in comparison with the other counterparts (PSO, HHO, or MRFO). By another means, the number of ranks where MPA approach generates a higher values of PV array power.
3) Calculate $R-$ that refers to the sum of ranks for runs in which the counterparts (PSO, HHO, or MRFO)

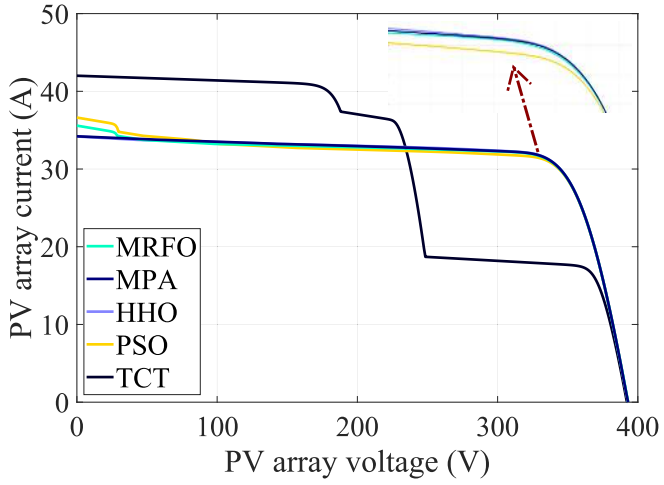


(a)

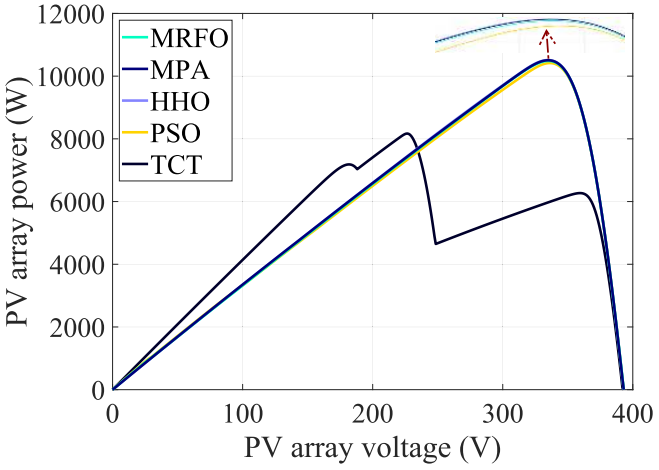


(b)

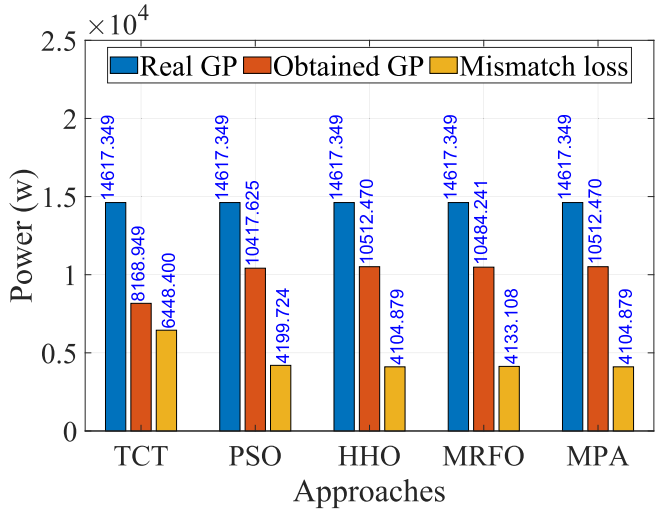


(c)

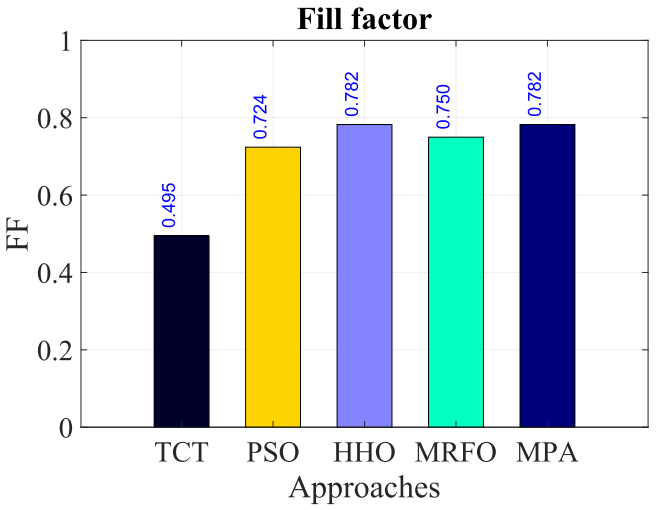


(d)

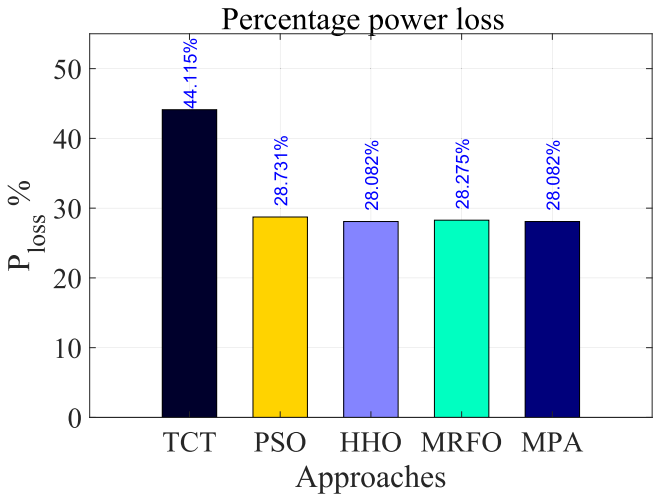


(e)

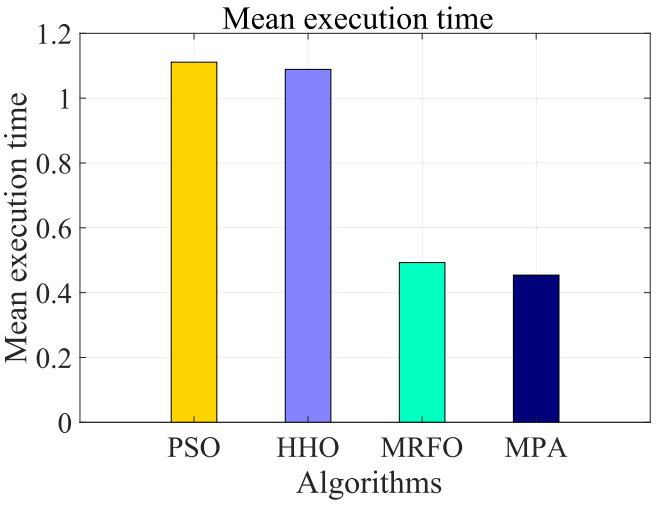


(f)

**FIGURE 7.** The algorithms approaches performances for pattern 1 based on (a) I-V characteristic, (b) P-V characteristic, (c) Miss-match power loss, (d) Fill factor, (e) percentage of power loss and (f) Execution time.

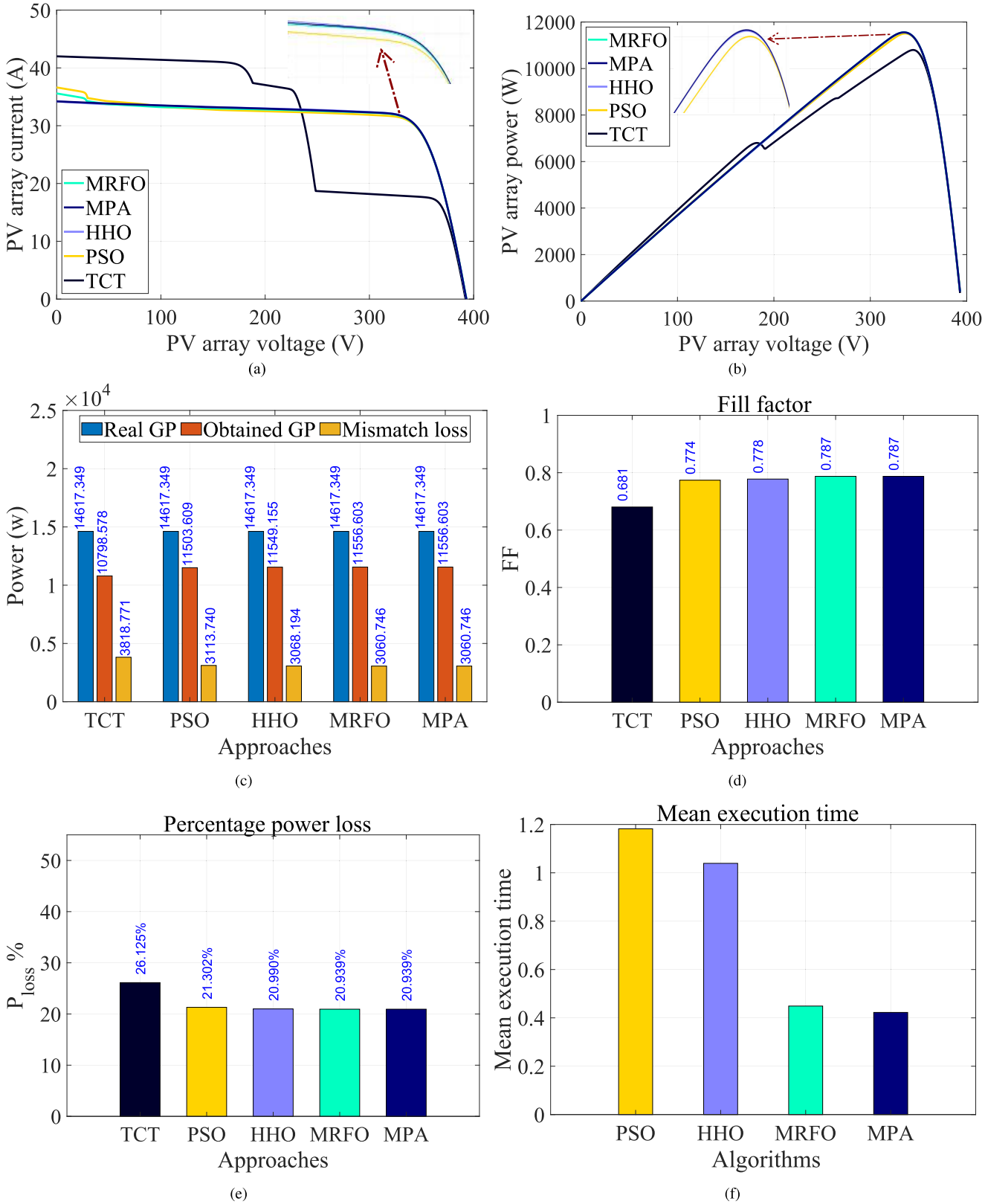


**FIGURE 8.** The algorithms approaches performances for pattern 2 based on (a) I-V characteristic, (b) P-V characteristic, (c) Miss-match power loss, (d) Fill factor, (e) percentage of power loss and (f) Execution time.

**TABLE 3.** Wilcoxon signed rank test results of MPA vs PSO, HHO, or MRFO for 9 × 9 PV array.

| Parameters | | | | | | | | |
|---|---|---|---|---|---|---|---|---|
| | Pattern 1 | | | | Pattern 2 | | | |
| | $R_+$ | $R_-$ | $p$-value | $H_0$ | $R_+$ | $R_-$ | $p$-value | $H_0$ |
| MPA vs PSO | 228.5000 | 24.5000 | 0.00073 | No | 105 | 0 | 0.00012 | No |
| MPA vs HHO | 423 | 12 | 0.00001 | No | 201.5000 | 8.50000 | 0.00012 | No |
| MPA vs MRFO | 240 | 13 | 0.00015 | No | 30 | 15 | 0.50781 | Yes |

**TABLE 4.** Analysis of TCT, PSO, HHO, MPA and MRFA for 16 × 16 PV array shade based on the objective function of Eq.6.

| TCT scheme | | | | PSO scheme | | | | HHO scheme | | | |
|---|---|---|---|---|---|---|---|---|---|---|---|
| $I_{Ri}$ | $I_R(A)$ | $V_m(V)$ | $P(W)$ | $I_{Ri}$ | $I_R(A)$ | $V_m(V)$ | $P(W)$ | $I_{Ri}$ | $I_R(A)$ | $V_m(V)$ | $P(W)$ |
| $I_{R1}$ | 12.4 $I_M$ | 16 $V_M$ | 198.4 $I_MV_M$ | $I_{R4}$ | 13.1 $I_M$ | 16 $V_M$ | 209.6 $I_MV_M$ | $I_{R5}$ | 13 $I_M$ | 16 $V_M$ | 208 $I_MV_M$ |
| $I_{R2}$ | 12.4 $I_M$ | 16 $V_M$ | 198.4 $I_MV_M$ | $I_{R5}$ | 13.1 $I_M$ | 16 $V_M$ | 209.6 $I_MV_M$ | $I_{R9}$ | 13 $I_M$ | 16 $V_M$ | 208 $I_MV_M$ |
| $I_{R3}$ | 12.4 $I_M$ | 16 $V_M$ | 198.4 $I_MV_M$ | $I_{R1}$ | 13.2 $I_M$ | 14 $V_M$ | 184.8 $I_MV_M$ | $I_{R10}$ | 13 $I_M$ | 16 $V_M$ | 208 $I_MV_M$ |
| $I_{R4}$ | 12.4 $I_M$ | 16 $V_M$ | 198.4 $I_MV_M$ | $I_{R3}$ | 13.2 $I_M$ | 14 $V_M$ | 184.8 $I_MV_M$ | $I_{R12}$ | 13 $I_M$ | 16 $V_M$ | 208 $I_MV_M$ |
| $I_{R5}$ | 13.2 $I_M$ | 12 $V_M$ | 158.4 $I_MV_M$ | $I_{R6}$ | 13.2 $I_M$ | 14 $V_M$ | 184.8 $I_MV_M$ | $I_{R16}$ | 13 $I_M$ | 16 $V_M$ | 208 $I_MV_M$ |
| $I_{R6}$ | 13.2 $I_M$ | 12 $V_M$ | 158.4 $I_MV_M$ | $I_{R7}$ | 13.2 $I_M$ | 14 $V_M$ | 184.8 $I_MV_M$ | $I_{R2}$ | 13.1 $I_M$ | 11 $V_M$ | 144.1 $I_MV_M$ |
| $I_{R7}$ | 13.2 $I_M$ | 12 $V_M$ | 158.4 $I_MV_M$ | $I_{R11}$ | 13.2 $I_M$ | 14 $V_M$ | 184.8 $I_MV_M$ | $I_{R6}$ | 13.1 $I_M$ | 11 $V_M$ | 144.1 $I_MV_M$ |
| $I_{R8}$ | 13.2 $I_M$ | 12 $V_M$ | 158.4 $I_MV_M$ | $I_{R14}$ | 13.2 $I_M$ | 14 $V_M$ | 184.8 $I_MV_M$ | $I_{R13}$ | 13.1 $I_M$ | 11 $V_M$ | 144.1 $I_MV_M$ |
| $I_{R9}$ | 13.6 $I_M$ | 8 $V_M$ | 108.8 $I_MV_M$ | $I_{R8}$ | 13.3 $I_M$ | 8 $V_M$ | 106.4 $I_MV_M$ | $I_{R1}$ | 13.2 $I_M$ | 8 $V_M$ | 105.6 $I_MV_M$ |
| $I_{R10}$ | 13.6 $I_M$ | 8 $V_M$ | 108.8 $I_MV_M$ | $I_{R12}$ | 13.3 $I_M$ | 8 $V_M$ | 106.4 $I_MV_M$ | $I_{R4}$ | 13.2 $I_M$ | 8 $V_M$ | 105.6 $I_MV_M$ |
| $I_{R11}$ | 13.6 $I_M$ | 8 $V_M$ | 108.8 $I_MV_M$ | $I_{R13}$ | 13.3 $I_M$ | 8 $V_M$ | 106.4 $I_MV_M$ | $I_{R14}$ | 13.3 $I_M$ | 6 $V_M$ | 79.8 $I_MV_M$ |
| $I_{R12}$ | 13.6 $I_M$ | 8 $V_M$ | 108.8 $I_MV_M$ | $I_{R15}$ | 13.3 $I_M$ | 8 $V_M$ | 106.4 $I_MV_M$ | $I_{R3}$ | 13.6 $I_M$ | 5 $V_M$ | 68 $I_MV_M$ |
| $I_{R13}$ | 14 $I_M$ | 4 $V_M$ | 56 $I_MV_M$ | $I_{R16}$ | 13.4 $I_M$ | 4 $V_M$ | 53.6 $I_MV_M$ | $I_{R8}$ | 13.6 $I_M$ | 5 $V_M$ | 68 $I_MV_M$ |
| $I_{R14}$ | 14 $I_M$ | 4 $V_M$ | 56 $I_MV_M$ | $I_{R9}$ | 13.5 $I_M$ | 3 $V_M$ | 40.5 $I_MV_M$ | $I_{R7}$ | 13.8 $I_M$ | 3 $V_M$ | 41.4 $I_MV_M$ |
| $I_{R15}$ | 14 $I_M$ | 4 $V_M$ | 56 $I_MV_M$ | $I_{R10}$ | 13.5 $I_M$ | 3 $V_M$ | 40.5 $I_MV_M$ | $I_{R11}$ | 13.9 $I_M$ | 2 $V_M$ | 27.8 $I_MV_M$ |
| $I_{R16}$ | 14 $I_M$ | 4 $V_M$ | 56 $I_MV_M$ | $I_{R2}$ | 13.8 $I_M$ | 1 $V_M$ | 13.8 $I_MV_M$ | $I_{R15}$ | 13.9 $I_M$ | 2 $V_M$ | 27.8 $I_MV_M$ |
| **MRFO scheme** | | | | **MPA scheme** | | | | | | | |
| $I_{Ri}$ | $I_R(A)$ | $V_m(V)$ | $P(W)$ | $I_{Ri}$ | $I_R(A)$ | $V_m(V)$ | $P(W)$ | | | | |
| $I_{R5}$ | 13.1 $I_M$ | 16 $V_M$ | 209.6 $I_MV_M$ | $I_{R1}$ | 13.2 $I_M$ | 16 $V_M$ | 211.2 $I_MV_M$ | | | | |
| $I_{R8}$ | 13.1 $I_M$ | 16 $V_M$ | 209.6 $I_MV_M$ | $I_{R2}$ | 13.2 $I_M$ | 16 $V_M$ | 211.2 $I_MV_M$ | | | | |
| $I_{R10}$ | 13.1 $I_M$ | 16 $V_M$ | 209.6 $I_MV_M$ | $I_{R3}$ | 13.2 $I_M$ | 16 $V_M$ | 211.2 $I_MV_M$ | | | | |
| $I_{R12}$ | 13.1 $I_M$ | 16 $V_M$ | 209.6 $I_MV_M$ | $I_{R4}$ | 13.2 $I_M$ | 16 $V_M$ | 211.2 $I_MV_M$ | | | | |
| $I_{R16}$ | 13.1 $I_M$ | 16 $V_M$ | 209.6 $I_MV_M$ | $I_{R9}$ | 13.2 $I_M$ | 16 $V_M$ | 211.2 $I_MV_M$ | | | | |
| $I_{R2}$ | 13.2 $I_M$ | 11 $V_M$ | 145.2 $I_MV_M$ | $I_{R12}$ | 13.2 $I_M$ | 16 $V_M$ | 211.2 $I_MV_M$ | | | | |
| $I_{R4}$ | 13.2 $I_M$ | 11 $V_M$ | 145.2 $I_MV_M$ | $I_{R13}$ | 13.2 $I_M$ | 16 $V_M$ | 211.2 $I_MV_M$ | | | | |
| $I_{R11}$ | 13.2 $I_M$ | 11 $V_M$ | 145.2 $I_MV_M$ | $I_{R15}$ | 13.2 $I_M$ | 16 $V_M$ | 211.2 $I_MV_M$ | | | | |
| $I_{R15}$ | 13.2 $I_M$ | 11 $V_M$ | 145.2 $I_MV_M$ | $I_{R16}$ | 13.2 $I_M$ | 16 $V_M$ | 211.2 $I_MV_M$ | | | | |
| $I_{R6}$ | 13.3 $I_M$ | 7 $V_M$ | 93.1 $I_MV_M$ | $I_{R11}$ | 13.3 $I_M$ | 7 $V_M$ | 93.1 $I_MV_M$ | | | | |
| $I_{R13}$ | 13.4 $I_M$ | 6 $V_M$ | 80.4 $I_MV_M$ | $I_{R7}$ | 13.4 $I_M$ | 6 $V_M$ | 80.4 $I_MV_M$ | | | | |
| $I_{R1}$ | 13.5 $I_M$ | 5 $V_M$ | 67.5 $I_MV_M$ | $I_{R8}$ | 13.4 $I_M$ | 6 $V_M$ | 80.4 $I_MV_M$ | | | | |
| $I_{R9}$ | 13.5 $I_M$ | 5 $V_M$ | 67.5 $I_MV_M$ | $I_{R10}$ | 13.4 $I_M$ | 6 $V_M$ | 80.4 $I_MV_M$ | | | | |
| $I_{R3}$ | 13.6 $I_M$ | 3 $V_M$ | 40.8 $I_MV_M$ | $I_{R5}$ | 13.5 $I_M$ | 3 $V_M$ | 40.5 $I_MV_M$ | | | | |
| $I_{R7}$ | 13.6 $I_M$ | 3 $V_M$ | 40.8 $I_MV_M$ | $I_{R6}$ | 13.5 $I_M$ | 3 $V_M$ | 40.5 $I_MV_M$ | | | | |
| $I_{R14}$ | 13.6 $I_M$ | 3 $V_M$ | 40.8 $I_MV_M$ | $I_{R14}$ | 13.5 $I_M$ | 3 $V_M$ | 40.5 $I_MV_M$ | | | | |

outperforms MPA. By another means, the number of ranks where MPA approach provides a lower values of PV array power.

4) The $p$-value is calculated to reveal the significance difference among the proposed approaches in a statistical hypothesis test. The smaller the $p$-value, the stronger evidences against the null hypothesis (reject null hypothesis, discovering a significant difference among the pairwise compared algorithms).

In this work, null hypothesis is valid when $H_0 =$ 'Yes', with a significance level = 0.05 ($p$-value > 0.05), that indicates no significant difference between the compared techniques in the performance (both have the same behavior). While if $H_0 =$ 'No', there is a significant difference between the techniques ($p$-value < 0.05).

Table. 3 summarizes the $R+$, $R-$, $p$-value and $H_0$ values. As illustrated from the table, the MPA approach exposes a significant improvements in comparison with PSO, HHO, and MRFO where the number of ranks where the MPA shows success in providing the highest values of PV array power more consistent than the other algorithms. As the $p-values$ are less than 0.05 (null-hypothesis is rejected), and the number of ranks where MPA outperforms the other peers is the largest ($R+ > R-$), we can conclude that there is a significant difference among the proposed algorithms in a

**TABLE 5.** Wilcoxon signed rank test results of MPA vs PSO, HHO, or MRFO for 16 × 16 PV array.

| Parameters | | | | |
|---|---|---|---|---|
| | Pattern 1 | | | |
| | $R_+$ | $R_-$ | $p$-value | $H_0$ |
| MPA vs PSO | 243 | 10 | 0.00012 | No |
| MPA vs HHO | 378 | 0 | $4.6823e-06$ | No |
| MPA vs MRFO | 309.5000 | 15.5000 | 0.00006 | No |

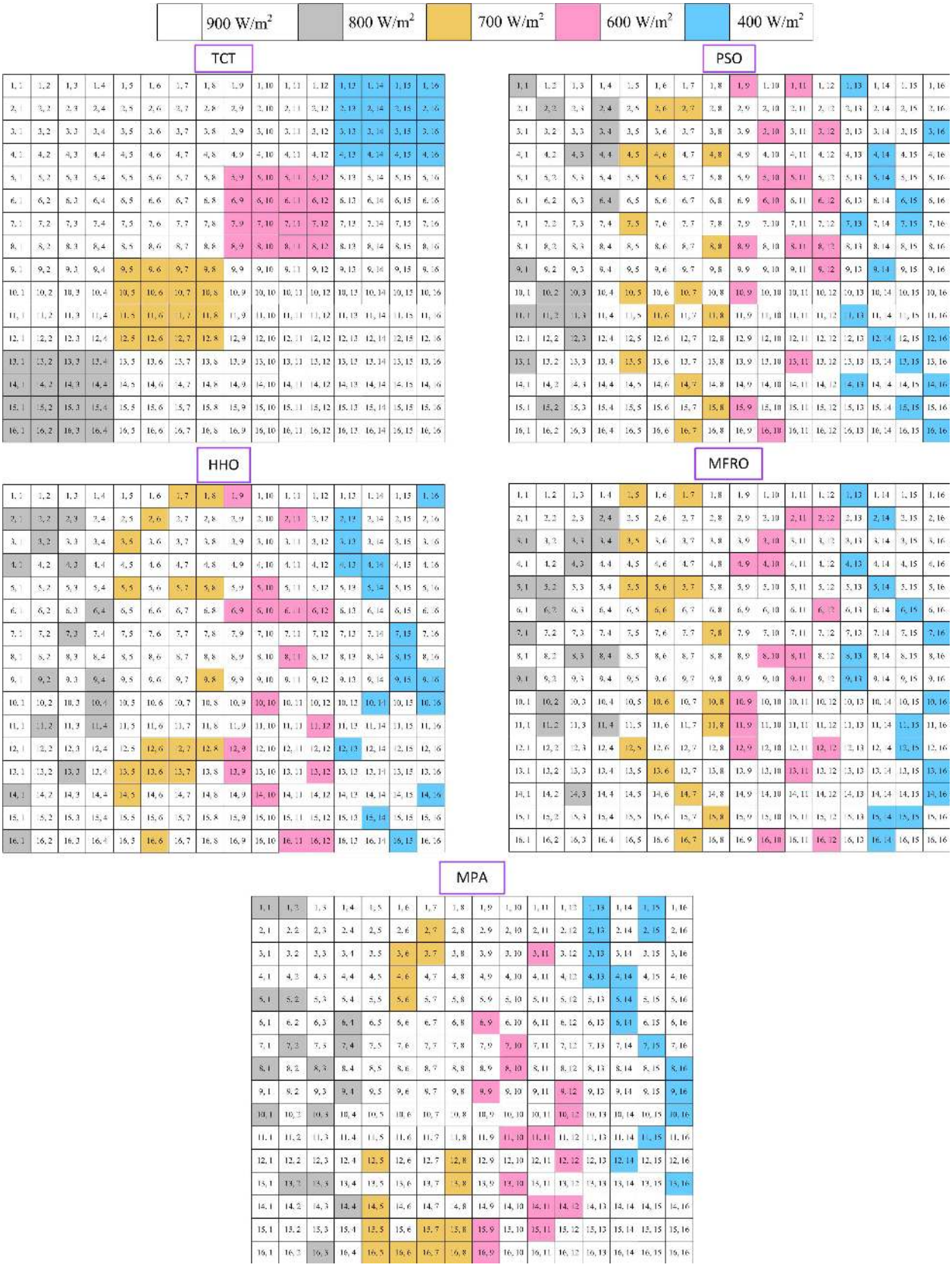


**FIGURE 9.** PV array arrangement based on, TCT, PSO, HHO, MRFO, and MPA for 16 × 16 PV array.

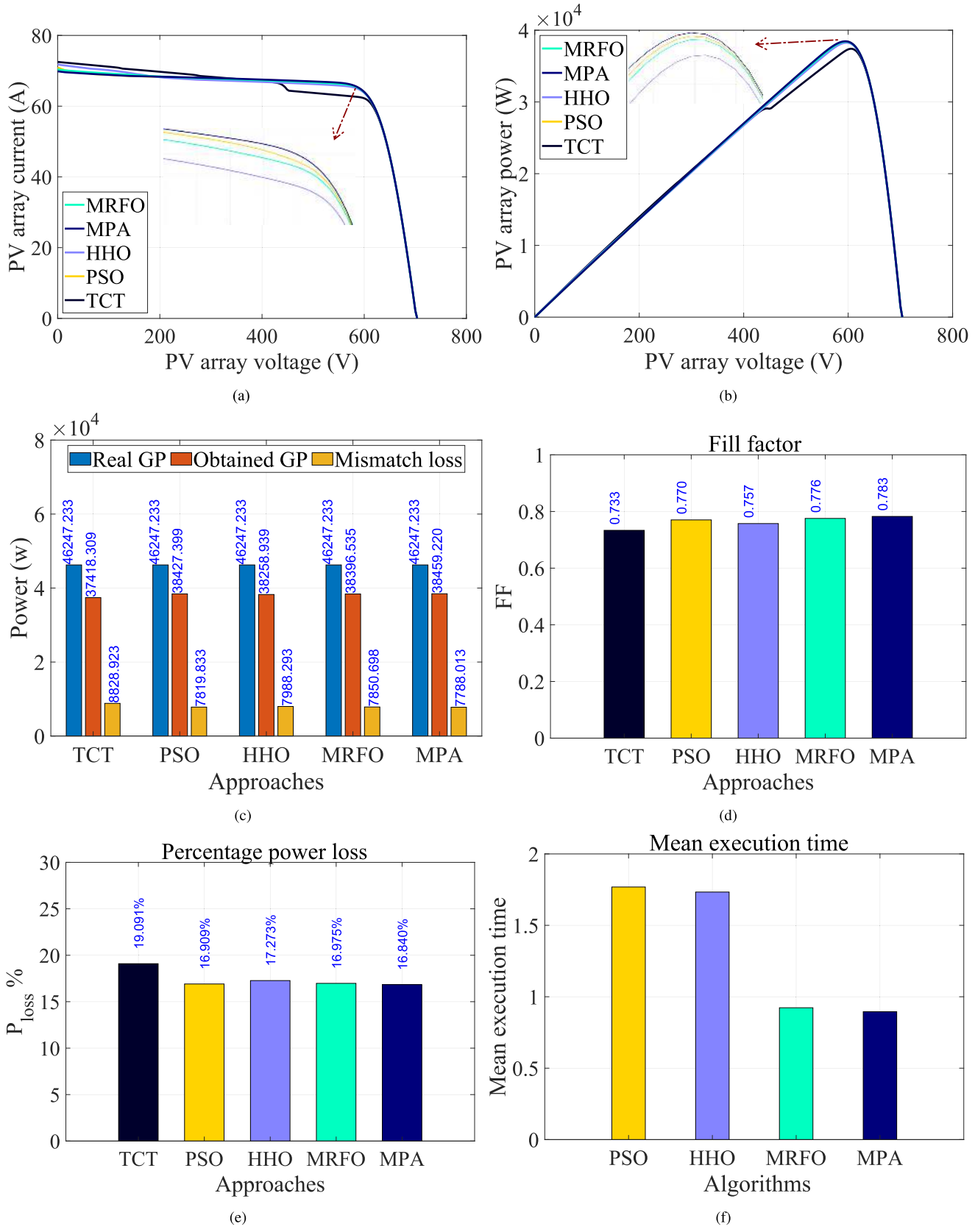


**FIGURE 10.** The algorithms approaches performances for 16 × 16 PV array (a) I-V characteristic, (b) P-V characteristic, (c) Miss-match power loss, (d) Fill factor, (e) percentage of power loss and (f) Execution time.

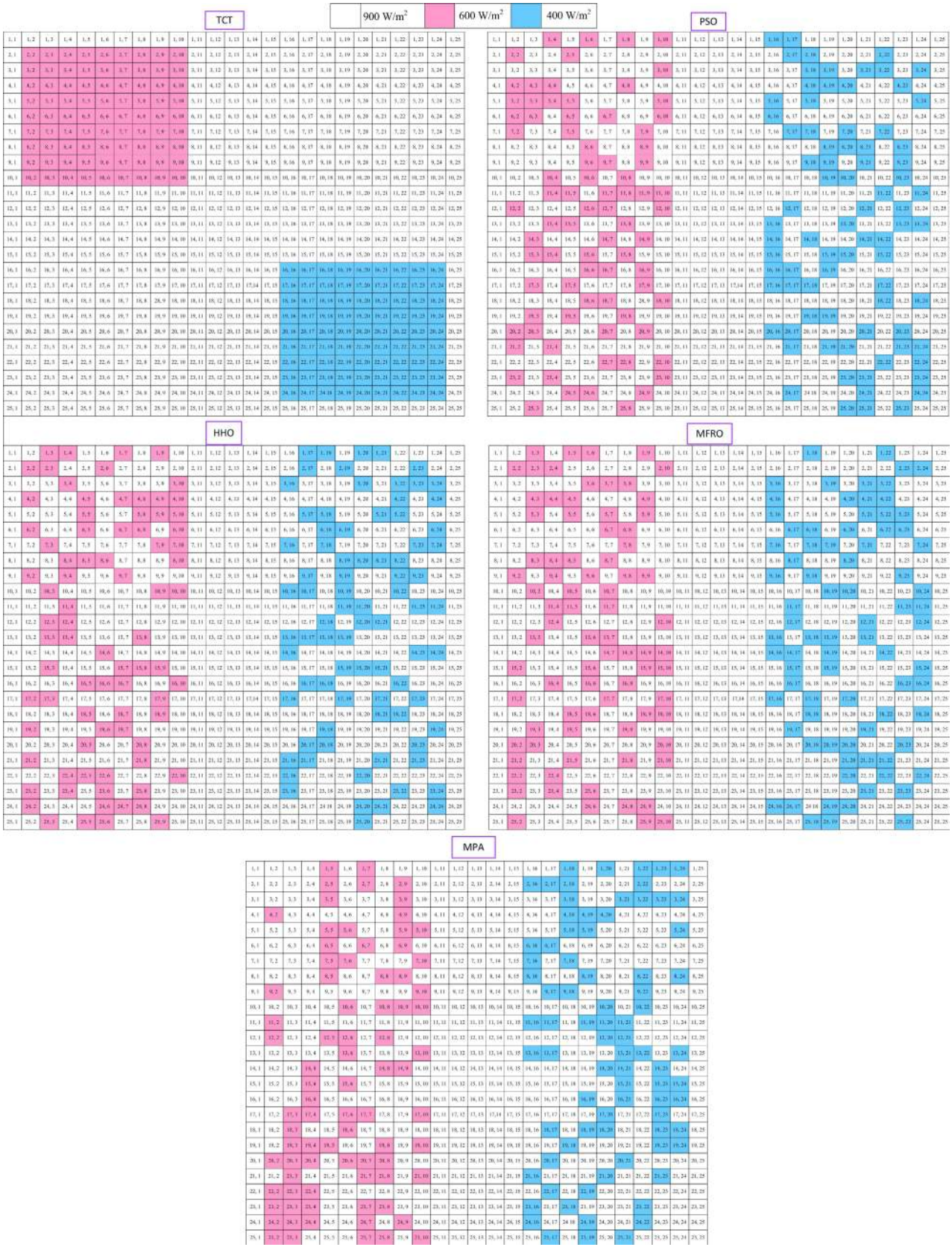


**FIGURE 11.** PV array arrangement based on, TCT, PSO, HHO, MRFO, and MPA for 25 × 25 PV array.

**TABLE 6.** Analysis of TCT, PSO, HHO, MPA and MRFA for 25 × 25 PV array shade based on the objective function of Eq.6.

| TCT scheme | | | | PSO scheme | | | | HHO scheme | | | |
|---|---|---|---|---|---|---|---|---|---|---|---|
| $I_{Ri}$ | $I_R(A)$ | $V_m(V)$ | $P(W)$ | $I_{Ri}$ | $I_R(A)$ | $V_m(V)$ | $P(W)$ | $I_{Ri}$ | $I_R(A)$ | $V_m(V)$ | $P(W)$ |
| $I_{R16}$ | 18 $I_M$ | 25 $V_M$ | 450 $I_MV_M$ | $I_{R4}$ | 19.3 $I_M$ | 25 $V_M$ | 482.5 $I_MV_M$ | $I_{R1}$ | 19.3 $I_M$ | 25 $V_M$ | 482.5 $I_MV_M$ |
| $I_{R17}$ | 18 $I_M$ | 25 $V_M$ | 450 $I_MV_M$ | $I_{R15}$ | 19.3 $I_M$ | 25 $V_M$ | 482.5 $I_MV_M$ | $I_{R5}$ | 19.3 $I_M$ | 25 $V_M$ | 482.5 $I_MV_M$ |
| $I_{R18}$ | 18 $I_M$ | 25 $V_M$ | 450 $I_MV_M$ | $I_{R20}$ | 19.3 $I_M$ | 25 $V_M$ | 482.5 $I_MV_M$ | $I_{R8}$ | 19.3 $I_M$ | 25 $V_M$ | 482.5 $I_MV_M$ |
| $I_{R19}$ | 18 $I_M$ | 25 $V_M$ | 450 $I_MV_M$ | $I_{R21}$ | 19.4 $I_M$ | 22 $V_M$ | 426.8 $I_MV_M$ | $I_{R3}$ | 19.4 $I_M$ | 22 $V_M$ | 426.8 $I_MV_M$ |
| $I_{R20}$ | 18 $I_M$ | 25 $V_M$ | 450 $I_MV_M$ | $I_{R5}$ | 19.5 $I_M$ | 21 $V_M$ | 409.5 $I_MV_M$ | $I_{R6}$ | 19.5 $I_M$ | 21 $V_M$ | 409.5 $I_MV_M$ |
| $I_{R21}$ | 18 $I_M$ | 25 $V_M$ | 450 $I_MV_M$ | $I_{R7}$ | 19.6 $I_M$ | 20 $V_M$ | 392 $I_MV_M$ | $I_{R7}$ | 19.6 $I_M$ | 20 $V_M$ | 392 $I_MV_M$ |
| $I_{R22}$ | 18 $I_M$ | 25 $V_M$ | 450 $I_MV_M$ | $I_{R9}$ | 19.6 $I_M$ | 20 $V_M$ | 392 $I_MV_M$ | $I_{R9}$ | 19.6 $I_M$ | 20 $V_M$ | 392 $I_MV_M$ |
| $I_{R23}$ | 18 $I_M$ | 25 $V_M$ | 450 $I_MV_M$ | $I_{R13}$ | 19.6 $I_M$ | 20 $V_M$ | 392 $I_MV_M$ | $I_{R10}$ | 19.6 $I_M$ | 20 $V_M$ | 392 $I_MV_M$ |
| $I_{R24}$ | 18 $I_M$ | 25 $V_M$ | 450 $I_MV_M$ | $I_{R14}$ | 19.6 $I_M$ | 20 $V_M$ | 392 $I_MV_M$ | $I_{R13}$ | 19.6 $I_M$ | 20 $V_M$ | 392 $I_MV_M$ |
| $I_{R2}$ | 19.8 $I_M$ | 16 $V_M$ | 316.8 $I_MV_M$ | $I_{R17}$ | 19.6 $I_M$ | 20 $V_M$ | 392 $I_MV_M$ | $I_{R17}$ | 19.6 $I_M$ | 20 $V_M$ | 392 $I_MV_M$ |
| $I_{R3}$ | 19.8 $I_M$ | 16 $V_M$ | 316.8 $I_MV_M$ | $I_{R3}$ | 19.7 $I_M$ | 15 $V_M$ | 295.5 $I_MV_M$ | $I_{R4}$ | 19.7 $I_M$ | 15 $V_M$ | 295.5 $I_MV_M$ |
| $I_{R4}$ | 19.8 $I_M$ | 16 $V_M$ | 316.8 $I_MV_M$ | $I_{R11}$ | 19.7 $I_M$ | 15 $V_M$ | 295.5 $I_MV_M$ | $I_{R15}$ | 19.8 $I_M$ | 14 $V_M$ | 277.2 $I_MV_M$ |
| $I_{R5}$ | 19.8 $I_M$ | 16 $V_M$ | 316.8 $I_MV_M$ | $I_{R12}$ | 19.8 $I_M$ | 13 $V_M$ | 257.4 $I_MV_M$ | $I_{R16}$ | 19.8 $I_M$ | 14 $V_M$ | 277.2 $I_MV_M$ |
| $I_{R6}$ | 19.8 $I_M$ | 16 $V_M$ | 316.8 $I_MV_M$ | $I_{R8}$ | 19.9 $I_M$ | 12 $V_M$ | 238.8 $I_MV_M$ | $I_{R23}$ | 19.8 $I_M$ | 14 $V_M$ | 277.2 $I_MV_M$ |
| $I_{R7}$ | 19.8 $I_M$ | 16 $V_M$ | 316.8 $I_MV_M$ | $I_{R10}$ | 20.1 $I_M$ | 11 $V_M$ | 221.1 $I_MV_M$ | $I_{R24}$ | 19.8 $I_M$ | 14 $V_M$ | 277.2 $I_MV_M$ |
| $I_{R8}$ | 19.8 $I_M$ | 16 $V_M$ | 316.8 $I_MV_M$ | $I_{R16}$ | 20.1 $I_M$ | 11 $V_M$ | 221.1 $I_MV_M$ | $I_{R21}$ | 19.9 $I_M$ | 10 $V_M$ | 199 $I_MV_M$ |
| $I_{R9}$ | 19.8 $I_M$ | 16 $V_M$ | 316.8 $I_MV_M$ | $I_{R23}$ | 20.1 $I_M$ | 11 $V_M$ | 221.1 $I_MV_M$ | $I_{R2}$ | 20.1 $I_M$ | 9 $V_M$ | 180.9 $I_MV_M$ |
| $I_{R10}$ | 19.8 $I_M$ | 16 $V_M$ | 316.8 $I_MV_M$ | $I_{R24}$ | 20.1 $I_M$ | 11 $V_M$ | 221.1 $I_MV_M$ | $I_{R11}$ | 20.2 $I_M$ | 8 $V_M$ | 161.6 $I_MV_M$ |
| $I_{R1}$ | 22.5 $I_M$ | 7 $V_M$ | 157.5 $I_MV_M$ | $I_{R1}$ | 20.3 $I_M$ | 7 $V_M$ | 142.1 $I_MV_M$ | $I_{R22}$ | 20.3 $I_M$ | 7 $V_M$ | 142.1 $I_MV_M$ |
| $I_{R11}$ | 22.5 $I_M$ | 7 $V_M$ | 157.5 $I_MV_M$ | $I_{R2}$ | 20.4 $I_M$ | 6 $V_M$ | 122.4 $I_MV_M$ | $I_{R12}$ | 20.4 $I_M$ | 6 $V_M$ | 122.4 $I_MV_M$ |
| $I_{R12}$ | 22.5 $I_M$ | 7 $V_M$ | 157.5 $I_MV_M$ | $I_{R25}$ | 20.4 $I_M$ | 6 $V_M$ | 122.4 $I_MV_M$ | $I_{R20}$ | 20.4 $I_M$ | 6 $V_M$ | 122.4 $I_MV_M$ |
| $I_{R13}$ | 22.5 $I_M$ | 7 $V_M$ | 157.5 $I_MV_M$ | $I_{R6}$ | 20.5 $I_M$ | 4 $V_M$ | 82 $I_MV_M$ | $I_{R18}$ | 20.6 $I_M$ | 4 $V_M$ | 82.4 $I_MV_M$ |
| $I_{R14}$ | 22.5 $I_M$ | 7 $V_M$ | 157.5 $I_MV_M$ | $I_{R18}$ | 20.6 $I_M$ | 3 $V_M$ | 61.8 $I_MV_M$ | $I_{R19}$ | 20.6 $I_M$ | 4 $V_M$ | 82.4 $I_MV_M$ |
| $I_{R15}$ | 22.5 $I_M$ | 7 $V_M$ | 157.5 $I_MV_M$ | $I_{R19}$ | 20.6 $I_M$ | 3 $V_M$ | 61.8 $I_MV_M$ | $I_{R14}$ | 20.7 $I_M$ | 2 $V_M$ | 41.4 $I_MV_M$ |
| $I_{R25}$ | 22.5 $I_M$ | 7 $V_M$ | 157.5 $I_MV_M$ | $I_{R22}$ | 20.6 $I_M$ | 3 $V_M$ | 61.8 $I_MV_M$ | $I_{R25}$ | 20.8 $I_M$ | 1 $V_M$ | 20.8 $I_MV_M$ |

| MRFO scheme | | | | MPA scheme | | | |
|---|---|---|---|---|---|---|---|
| $I_{Ri}$ | $I_R(A)$ | $V_m(V)$ | $P(W)$ | $I_{Ri}$ | $I_R(A)$ | $V_m(V)$ | $P(W)$ |
| $I_{R4}$ | 19.3 $I_M$ | 25 $V_M$ | 482.5 $I_MV_M$ | $I_{R1}$ | 19.4 $I_M$ | 25 $V_M$ | 485 $I_MV_M$ |
| $I_{R5}$ | 19.3 $I_M$ | 25 $V_M$ | 482.5 $I_MV_M$ | $I_{R3}$ | 19.4 $I_M$ | 25 $V_M$ | 485 $I_MV_M$ |
| $I_{R14}$ | 19.3 $I_M$ | 25 $V_M$ | 482.5 $I_MV_M$ | $I_{R13}$ | 19.4 $I_M$ | 25 $V_M$ | 485 $I_MV_M$ |
| $I_{R6}$ | 19.4 $I_M$ | 22 $V_M$ | 426.8 $I_MV_M$ | $I_{R18}$ | 19.4 $I_M$ | 25 $V_M$ | 485 $I_MV_M$ |
| $I_{R9}$ | 19.5 $I_M$ | 21 $V_M$ | 409.5 $I_MV_M$ | $I_{R19}$ | 19.5 $I_M$ | 21 $V_M$ | 409.5 $I_MV_M$ |
| $I_{R3}$ | 19.6 $I_M$ | 20 $V_M$ | 392 $I_MV_M$ | $I_{R23}$ | 19.5 $I_M$ | 21 $V_M$ | 409.5 $I_MV_M$ |
| $I_{R13}$ | 19.6 $I_M$ | 20 $V_M$ | 392 $I_MV_M$ | $I_{R24}$ | 19.5 $I_M$ | 21 $V_M$ | 409.5 $I_MV_M$ |
| $I_{R20}$ | 19.6 $I_M$ | 20 $V_M$ | 392 $I_MV_M$ | $I_{R25}$ | 19.5 $I_M$ | 21 $V_M$ | 409.5 $I_MV_M$ |
| $I_{R24}$ | 19.6 $I_M$ | 20 $V_M$ | 392 $I_MV_M$ | $I_{R2}$ | 19.6 $I_M$ | 17 $V_M$ | 333.2 $I_MV_M$ |
| $I_{R7}$ | 19.7 $I_M$ | 16 $V_M$ | 315.2 $I_MV_M$ | $I_{R8}$ | 19.6 $I_M$ | 17 $V_M$ | 333.2 $I_MV_M$ |
| $I_{R15}$ | 19.8 $I_M$ | 15 $V_M$ | 297 $I_MV_M$ | $I_{R11}$ | 19.7 $I_M$ | 15 $V_M$ | 295.5 $I_MV_M$ |
| $I_{R18}$ | 19.8 $I_M$ | 15 $V_M$ | 297 $I_MV_M$ | $I_{R20}$ | 19.7 $I_M$ | 15 $V_M$ | 295.5 $I_MV_M$ |
| $I_{R21}$ | 19.8 $I_M$ | 15 $V_M$ | 297 $I_MV_M$ | $I_{R5}$ | 19.8 $I_M$ | 13 $V_M$ | 257.4 $I_MV_M$ |
| $I_{R10}$ | 20.1 $I_M$ | 12 $V_M$ | 241.2 $I_MV_M$ | $I_{R21}$ | 19.8 $I_M$ | 13 $V_M$ | 257.4 $I_MV_M$ |
| $I_{R11}$ | 20.1 $I_M$ | 12 $V_M$ | 241.2 $I_MV_M$ | $I_{R17}$ | 20 $I_M$ | 11 $V_M$ | 220 $I_MV_M$ |
| $I_{R16}$ | 20.1 $I_M$ | 12 $V_M$ | 241.2 $I_MV_M$ | $I_{R14}$ | 20.1 $I_M$ | 10 $V_M$ | 201 $I_MV_M$ |
| $I_{R17}$ | 20.1 $I_M$ | 12 $V_M$ | 241.2 $I_MV_M$ | $I_{R16}$ | 20.2 $I_M$ | 9 $V_M$ | 181.8 $I_MV_M$ |
| $I_{R25}$ | 20.1 $I_M$ | 12 $V_M$ | 241.2 $I_MV_M$ | $I_{R10}$ | 20.3 $I_M$ | 8 $V_M$ | 162.4 $I_MV_M$ |
| $I_{R1}$ | 20.3 $I_M$ | 7 $V_M$ | 142.1 $I_MV_M$ | $I_{R12}$ | 20.3 $I_M$ | 8 $V_M$ | 162.4 $I_MV_M$ |
| $I_{R2}$ | 20.3 $I_M$ | 7 $V_M$ | 142.1 $I_MV_M$ | $I_{R4}$ | 20.4 $I_M$ | 6 $V_M$ | 122.4 $I_MV_M$ |
| $I_{R8}$ | 20.3 $I_M$ | 7 $V_M$ | 142.1 $I_MV_M$ | $I_{R9}$ | 20.4 $I_M$ | 6 $V_M$ | 122.4 $I_MV_M$ |
| $I_{R12}$ | 20.4 $I_M$ | 4 $V_M$ | 81.6 $I_MV_M$ | $I_{R15}$ | 20.4 $I_M$ | 6 $V_M$ | 122.4 $I_MV_M$ |
| $I_{R22}$ | 20.4 $I_M$ | 4 $V_M$ | 81.6 $I_MV_M$ | $I_{R6}$ | 20.6 $I_M$ | 3 $V_M$ | 61.8 $I_MV_M$ |
| $I_{R19}$ | 20.6 $I_M$ | 2 $V_M$ | 41.2 $I_MV_M$ | $I_{R7}$ | 20.6 $I_M$ | 3 $V_M$ | 61.8 $I_MV_M$ |
| $I_{R23}$ | 20.6 $I_M$ | 2 $V_M$ | 41.2 $I_MV_M$ | $I_{R22}$ | 20.6 $I_M$ | 3 $V_M$ | 61.8 $I_MV_M$ |

favor of MPA. For pattern 2, MPA and MRFO has the same performance.

## VII. EXTENSIVE ANALYSES WITH LARGE SCALE PV ARRAY

Two large scale of 16 × 16 and 25 × 25 PV arrays are considered in this part to evaluate the applicability of the proposed approach even for large scale PV plants. Implementation of proposed techniques for large scale PV plants proves the robustness and perfectness of the considered algorithms.

### A. THE 16 × 16 PV ARRAY

The surface of the shaded PV array receives four levels of sun radiation with the profile of $900W/m^2$, $800W/m^2$, $700W/m^2$, $600W/m^2$, and $400W/m^2$. The PV array in the TCT arrangement and the reconfigured schemes based on the proposed algorithms are illustrated in Fig. 9. The values of the row current values and corresponded voltage and power have been computed as listed in Table 4.

The reported results in Table 4 confirm that the MPA-based arrangement provides the highest value of the PV harvested power of 211.2 $I_m$ $V_m$ whilst the MRFO and PSO occupied the second rank with providing maximum power of

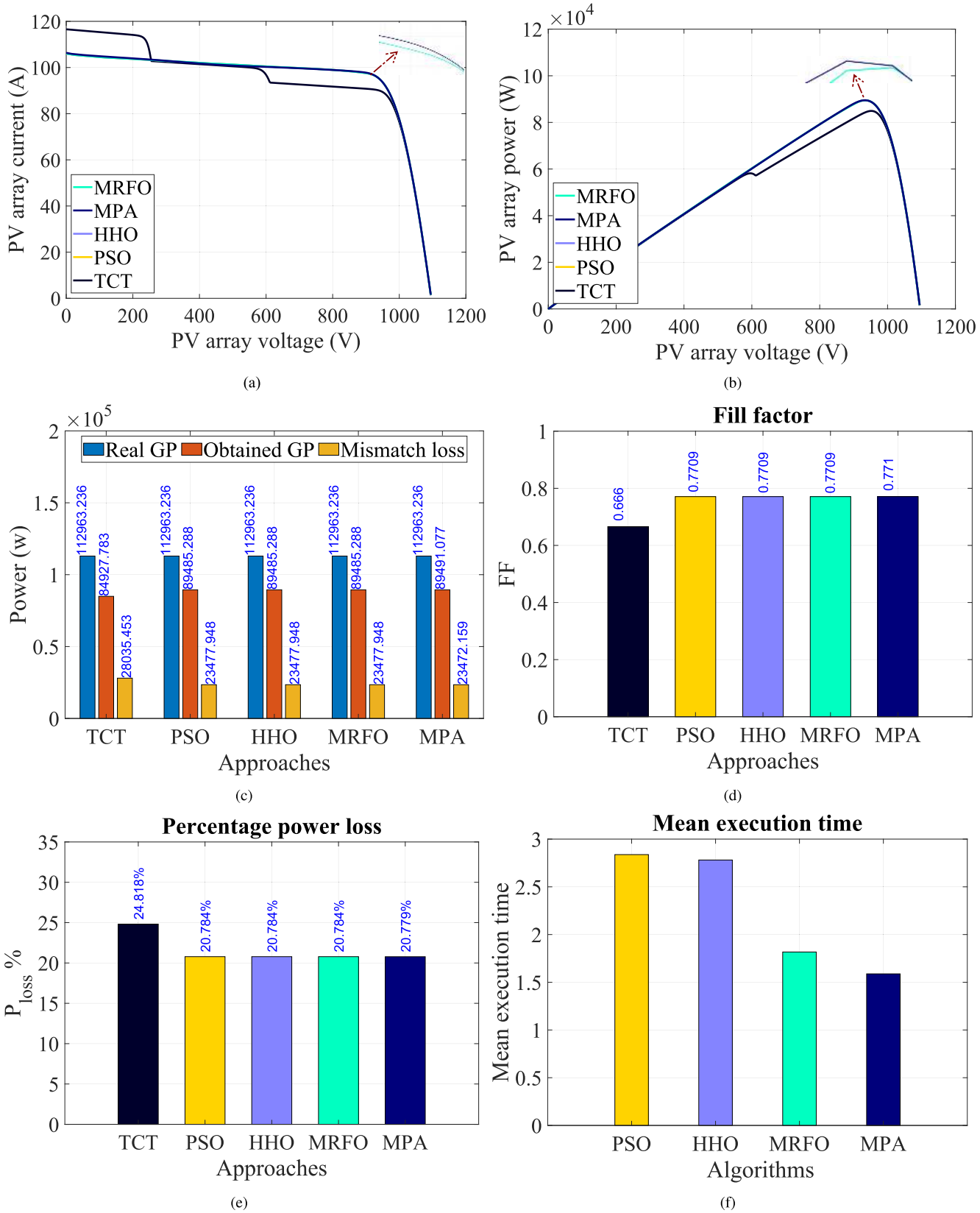


**FIGURE 12.** The algorithms approaches performances for 25 × 25 PV array (a) I-V characteristic, (b) P-V characteristic, (c) Miss-match power loss, (d) Fill factor, (e) percentage of power loss and (f) Execution time.

**TABLE 7. Wilcoxon signed rank test results of MPA vs PSO, HHO, or MRFO for 25 × 25 PV array.**

| Parameters | | | | |
|---|---|---|---|---|
| | Pattern 1 | | | |
| | $R_+$ | $R_-$ | $p$-value | $H_0$ |
| MPA vs PSO | 279.5 | 20.5 | 0.00019 | No |
| MPA vs HHO | 334.5 | 16.5 | 0.00005 | No |
| MPA vs MRFO | 255.5 | 69.5 | 0.01121 | No |

209.6 $I_m$ $V_m$. HHO-scheme achieves maximum power of 208 $I_m$ $V_m$ and TCT connection exposes maximum power of 198.4 $I_m$ $V_m$, consequently the TCT is not the efficient approach for the shaded large scale PV array. By inspecting the I-V and P-V characteristics of Figs. 10(a) - 10(b), respectively one can recognize that MPA-approach tackled the multi-peak issue with harvesting the highest PV power. The bar plots of the mismatch power loss, fill factor (FF), percentage power loss of Figs. 10(c) - 10(d) and 10(e) expose that MPA-arrangement minimizes the value of the mismatch power loss with percentage of 11.8 % in comparison with TCT connection (where $\frac{(8828.925-7788.013)*100}{8828.925} = 11.8\%$), sequentially it has the highest FF value and lowest percentage power loss of 0.783 and 16.840%, respectively (see Figs. 10(d) - and 10(e)). Whereas the MRFO, HHO, PSO and TCT-arrangements achieve percentage power loss of 16.975%, 17.273%, 16.909%, and 19.09% respectively. For the mean execution time of Fig. 10(f), MPA has the least value in comparison with PSO, HHO and MRFO. Therefore, MPA can recommend successfully for large scale PV re configuring system.

To intensively investigate the MPA performance the Wilcoxon signed rank test has been computed as in Table. 5 among the proposed algorithms to clarify the reliability of the MPA technique. The $R+$, $R-$, and $p$-value prove the superiority of MPA in providing the consistent results across the number of independent runs consequently the null-hypothesise has been rejected. At this end MPA confirms its quality not only in producing the highest PV power and solving the multi-peak issue but also in achieving the highest consistent solutions.

### B. THE 25 × 25 PV ARRAY

In the purpose of investigating the performance of the proposed approach with a more complicated system, a shaded PV array with a scale of 25 × 25 has been considered. The surface of the studied array receives sun radiation at the levels of $900W/m^2$, $600W/m^2$, and $400W/m^2$. The MPA, MRFO, HHO, PSO are implemented to disperse the shadow levels on the PV surface regularly to reinforce the produced PV power of the array. The row current, voltage, and power values are reported in Table. 6 regarding for the obtained patterns in Fig. 11. THe harvested PV power value based on MPA reconfiguration pattern is the highest value in comparison with MRFO, HHO, PSO and TCT arrangements where it is 485 $I_M V_M$ whereas the other meta-heuristic peers provides 482.5 $I_M V_M$ and TCT connection offers 450 $I_M V_M$. For the obtained I-V curves of Fig. 12(a) and P-V curves of Fig 12(b), the MPA scheme tackled the appearing multi-peaks issue in the obtained curves with high FF and minimum power loss and mismatch power in comparison with the other counterparts as illustrated in Figs. 12(d), 12(e) and 12(c). For evaluating the reliability of the MPA in providing the robust and consistent solutions in comparison with MRFO, HHO and PSO, the Wilcoxon signed rank has been performed as in Table. 7. The reported $R_+$, $R_-$, $p$-value reveal the superiority of the proposed MPA approach with a significant difference from the other counterparts.

According for the early mentioned discussion, the MPA proves its efficiency and superiority not only with scale of 9 × 9 PV array but also with the largest scale of 25 × 25 PV array as well.

## VIII. CONCLUSION

A regular distribution of the shadow on the surface of the shaded PV array buttresses the array harvested power. Therefore, in this paper, authors proposed an innovated objective function with robust and reliable optimization algorithm named marine predators algorithm (MPA) to provide the optimal pattern structure for three dimensions of PV arrays which are 9 × 9, 16 × 16 and 25 × 25. The MPA is tested with several shade patterns and compared with manta ray foraging optimization (MRFO), Harris hawk optimizer (HHO) and particle swarm optimizer (PSO) as well as the total-cross-tied (TCT) connection. Several quality and statistical measures are computed such as mismatch power loss, fill factor, percentage power loss as well as Wilcoxon signed rank test to assess the performance of the proposed approach. The I-V and P-V characteristics have been exhibited to investigate the applicability of the proposed MPA in comparison with the other counterparts. Moreover, the mean execution time has been evaluated. The results reveal that MPA enhanced the PV array power by percentage of 28.6 %, 2.7 % and 5.7 % in cases of 9 × 9, 16 × 16 and 25 × 25 PV arrays, respectively and a uni-peak PV characterises is achieved as well with lowest execution time and highest consistency in the results across the number of independent runs. Therefore, authors recommend MPA as an efficient and applicable algorithm for PV reconfiguration system at any dimension of PV array structures.

## REFERENCES

[1] A. Fathy, "Recent meta-heuristic grasshopper optimization algorithm for optimal reconfiguration of partially shaded PV array," *Sol. Energy*, vol. 171, pp. 638–651, Sep. 2018.

[2] K. Sangeetha, T. S. Babu, and N. Rajasekar, "Fireworks algorithm-based maximum power point tracking for uniform irradiation as well as under partial shading condition," in *Artificial Intelligence and Evolutionary Computations in Engineering Systems*. Springer, India, 2016, pp. 79–88.

[3] N. Kaushika and A. Rai, "An investigation of mismatch losses in solar photovoltaic cell networks," *Energy*, vol. 32, no. 5, pp. 755–759, May 2007.

[4] K. Saha, "Planning and installing photovoltaic system: A guide for installers, architects and engineers," *Int. J. Environ. Stud.*, 2nd edition, pp. 1–2, Sep. 2014.

[5] M. García, J. A. Vera, L. Marroyo, E. Lorenzo, and M. Pérez, "Solar-tracking PV plants in Navarra: A 10 MW assessment," *Prog. Photovoltaics, Res. Appl.*, vol. 17, no. 5, pp. 337–346, Aug. 2009.

[6] L. Xie, J. Qi, G. Weng, and Y. Zhang, "Multi-level PV inverter with photovoltaic groups independent MPPT control," in *Proc. 17th Int. Conf. Electr. Mach. Syst. (ICEMS)*, Oct. 2014, pp. 829–834.
[7] S. R. Pendem, S. Mikkili, and P. K. Bonthagorla, "PV distributed-MPP tracking: Total-cross-tied configuration of string-integrated-converters to extract the maximum power under various PSCs," *IEEE Syst. J.*, vol. 14, no. 1, pp. 1046–1057, Mar. 2020.
[8] A. Elmelegi, M. Aly, E. M. Ahmed, and A. G. Alharbi, "A simplified phase-shift PWM-based feedforward distributed MPPT method for grid-connected cascaded PV inverters," *Sol. Energy*, vol. 187, pp. 1–12, Jul. 2019.
[9] K. Sangeetha, T. Sudhakar Babu, N. Sudhakar, and N. Rajasekar, "Modeling, analysis and design of efficient maximum power extraction method for solar PV system," *Sustain. Energy Technol. Assessments*, vol. 15, pp. 60–70, Jun. 2016.
[10] T. Sudhakar Babu, N. Rajasekar, and K. Sangeetha, "Modified particle swarm optimization technique based maximum power point tracking for uniform and under partial shading condition," *Appl. Soft Comput.*, vol. 34, pp. 613–624, Sep. 2015.
[11] T. Sudhakar Babu, K. Sangeetha, and N. Rajasekar, "Voltage band based improved particle swarm optimization technique for maximum power point tracking in solar photovoltaic system," *J. Renew. Sustain. Energy*, vol. 8, no. 1, Jan. 2016, Art. no. 013106.
[12] M. Vysakh, M. Azharuddin, H. Vilas, K. Muralidhar, D. Paul, B. Jacob, and N. Rajasekar, "Maximum power point tracking using modified PSO with CUK Converter," in *Proc. Int. Conf. Adv. Electr. Eng. (ICAEE)*, Jan. 2014, pp. 1–6.
[13] A. I. Bratcu, I. Munteanu, S. Bacha, D. Picault, and B. Raison, "Cascaded DC–DC converter photovoltaic systems: Power optimization issues," *IEEE Trans. Ind. Electron.*, vol. 58, no. 2, pp. 403–411, Feb. 2011.
[14] G. Velasco-Quesada, F. Guinjoan-Gispert, R. Piqué-López, M. Román-Lumbreras, and A. Conesa-Roca, "Electrical PV array reconfiguration strategy for energy extraction improvement in grid-connected PV systems," *IEEE Trans. Ind. Electron.*, vol. 56, no. 11, pp. 4319–4331, Nov. 2009.
[15] S. Malathy and R. Ramaprabha, "Reconfiguration strategies to extract maximum power from photovoltaic array under partially shaded conditions," *Renew. Sustain. Energy Rev.*, vol. 81, pp. 2922–2934, Jan. 2018.
[16] S. N. Deshkar, S. B. Dhale, J. S. Mukherjee, T. S. Babu, and N. Rajasekar, "Solar PV array reconfiguration under partial shading conditions for maximum power extraction using genetic algorithm," *Renew. Sustain. Energy Rev.*, vol. 43, pp. 102–110, Mar. 2015.
[17] Y.-J. Wang and P.-C. Hsu, "An investigation on partial shading of PV modules with different connection configurations of PV cells," *Energy*, vol. 36, no. 5, pp. 3069–3078, May 2011.
[18] N. K. Gautam and N. D. Kaushika, "Reliability evaluation of solar photovoltaic arrays," *Sol. Energy*, vol. 72, no. 2, pp. 129–141, Feb. 2002.
[19] O. Bingöl and B. Özkaya, "Analysis and comparison of different PV array configurations under partial shading conditions," *Sol. Energy*, vol. 160, pp. 336–343, Jan. 2018.
[20] M. Z. Shams El-Dein, M. Kazerani, and M. M. A. Salama, "Optimal photovoltaic array reconfiguration to reduce partial shading losses," *IEEE Trans. Sustain. Energy*, vol. 4, no. 1, pp. 145–153, Jan. 2013.
[21] D. Nguyen and B. Lehman, "An adaptive solar photovoltaic array using model-based reconfiguration algorithm," *IEEE Trans. Ind. Electron.*, vol. 55, no. 7, pp. 2644–2654, Jul. 2008.
[22] B. I. Rani, G. S. Ilango, and C. Nagamani, "Enhanced power generation from PV array under partial shading conditions by shade dispersion using su do ku configuration," *IEEE Trans. Sustain. Energy*, vol. 4, no. 3, pp. 594–601, Jul. 2013.
[23] S. G. Krishna and T. Moger, "Optimal SuDoKu reconfiguration technique for total-cross-tied PV array to increase power output under non-uniform irradiance," *IEEE Trans. Energy Convers.*, vol. 34, no. 4, pp. 1973–1984, Dec. 2019.
[24] H. S. Sahu, S. K. Nayak, and S. Mishra, "Maximizing the power generation of a partially shaded PV array," *IEEE J. Emerg. Sel. Topics Power Electron.*, vol. 4, no. 2, pp. 626–637, Jun. 2016.
[25] B. Dhanalakshmi and N. Rajasekar, "A novel competence square based PV array reconfiguration technique for solar PV maximum power extraction," *Energy Convers. Manage.*, vol. 174, pp. 897–912, Oct. 2018.
[26] B. Dhanalakshmi and N. Rajasekar, "Dominance square based array reconfiguration scheme for power loss reduction in solar PhotoVoltaic (PV) systems," *Energy Convers. Manage.*, vol. 156, pp. 84–102, Jan. 2018.
[27] S. Vijayalekshmy, G. R. Bindu, and S. R. Iyer, "A novel Zig-Zag scheme for power enhancement of partially shaded solar arrays," *Sol. Energy*, vol. 135, pp. 92–102, Oct. 2016.
[28] P. R. Satpathy and R. Sharma, "Power and mismatch losses mitigation by a fixed electrical reconfiguration technique for partially shaded photovoltaic arrays," *Energy Convers. Manage.*, vol. 192, pp. 52–70, Jul. 2019.
[29] M. Akrami and K. Pourhossein, "A novel reconfiguration procedure to extract maximum power from partially-shaded photovoltaic arrays," *Sol. Energy*, vol. 173, pp. 110–119, Oct. 2018.
[30] M. Horoufiany and R. Ghandehari, "Optimal fixed reconfiguration scheme for PV arrays power enhancement under mutual shading conditions," *IET Renew. Power Gener.*, vol. 11, no. 11, pp. 1456–1463, Sep. 2017.
[31] I. Nasiruddin, S. Khatoon, M. F. Jalil, and R. C. Bansal, "Shade diffusion of partial shaded PV array by using odd-even structure," *Sol. Energy*, vol. 181, pp. 519–529, Mar. 2019.
[32] P. R. Satpathy, R. Sharma, and S. Dash, "An efficient SD-PAR technique for maximum power generation from modules of partially shaded PV arrays," *Energy*, vol. 175, pp. 182–194, May 2019.
[33] M. Jazayeri, K. Jazayeri, and S. Uysal, "Adaptive photovoltaic array reconfiguration based on real cloud patterns to mitigate effects of non-uniform spatial irradiance profiles," *Sol. Energy*, vol. 155, pp. 506–516, Oct. 2017.
[34] P. D. S. Vicente, T. C. Pimenta, and E. R. Ribeiro, "Photovoltaic array reconfiguration strategy for maximization of energy production," *Int. J. Photoenergy*, vol. 2015, pp. 1–11, 2015.
[35] T. Ngo Ngoc, Q. N. Phung, L. N. Tung, E. R. Sanseverino, P. Romano, and F. Viola, "Increasing efficiency of photovoltaic systems under non-homogeneous solar irradiation using improved dynamic programming methods," *Sol. Energy*, vol. 150, pp. 325–334, Jul. 2017.
[36] T. S. Babu, J. P. Ram, T. Dragi ević, M. Miyatake, F. Blaabjerg, and N. Rajasekar, "Particle swarm optimization based solar PV array reconfiguration of the maximum power extraction under partial shading conditions," *IEEE Trans. Sustain. Energy*, vol. 9, no. 1, pp. 74–85, Jan. 2018.
[37] Q. Bai, "Analysis of particle swarm optimization algorithm," *Comput. Inf. Sci.*, vol. 3, no. 1, p. 180, Jan. 2010.
[38] D. Yousri, D. Allam, and M. B. Eteiba, "Optimal photovoltaic array reconfiguration for alleviating the partial shading influence based on a modified harris hawks optimizer," *Energy Convers. Manage.*, vol. 206, Feb. 2020, Art. no. 112470.
[39] M. Azharuddin, T. S. Babu, N. Bilakanti, and N. Rajasekar, "A nearly accurate solar photovoltaic emulator using a dSPACE controller for real-time control," *Electr. Power Compon. Syst.*, vol. 44, no. 7, pp. 774–782, Apr. 2016.
[40] D. Yousri, S. B. Thanikanti, D. Allam, V. K. Ramachandaramurthy, and M. B. Eteiba, "Fractional chaotic ensemble particle swarm optimizer for identifying the single, double, and three diode photovoltaic models' parameters," *Energy*, vol. 195, Mar. 2020, Art. no. 116979.
[41] T. Sudhakar Babu, J. Prasanth Ram, K. Sangeetha, A. Laudani, and N. Rajasekar, "Parameter extraction of two diode solar PV model using fireworks algorithm," *Sol. Energy*, vol. 140, pp. 265–276, Dec. 2016.
[42] D. F. Alam, D. A. Yousri, and M. B. Eteiba, "Flower pollination algorithm based solar PV parameter estimation," *Energy Convers. Manage.*, vol. 101, pp. 410–422, Sep. 2015.
[43] D. Allam, D. A. Yousri, and M. B. Eteiba, "Parameters extraction of the three diode model for the multi-crystalline solar cell/module using moth-flame optimization algorithm," *Energy Convers. Manage.*, vol. 123, pp. 535–548, Sep. 2016.
[44] D. H. Wolpert and W. G. Macready, "No free lunch theorems for optimization," *IEEE Trans. Evol. Comput.*, vol. 1, no. 1, pp. 67–82, Apr. 1997.
[45] A. Faramarzi, M. Heidarinejad, S. Mirjalili, and A. H. Gandomi, "Marine predators algorithm: A nature-inspired Metaheuristic," *Expert Syst. Appl.*, vol. 152, Aug. 2020, Art. no. 113377.
[46] D. Yousri, D. Allam, and M. B. Eteiba, "Chaotic whale optimizer variants for parameters estimation of the chaotic behavior in permanent magnet synchronous motor," *Appl. Soft Comput.*, vol. 74, pp. 479–503, Jan. 2019.
[47] J. Derrac, S. García, D. Molina, and F. Herrera, "A practical tutorial on the use of nonparametric statistical tests as a methodology for comparing evolutionary and swarm intelligence algorithms," *Swarm Evol. Comput.*, vol. 1, no. 1, pp. 3–18, Mar. 2011.